LA-13254

UC-700
Issued: February 1997

Problems Encountered during Impact Calculations Using Analytic Equations of State

Jerry F. Kerrisk
*William B. Harvey**

**Consultant at Los Alamos. Western Atlas, 14000 Betka Rd., Hempstead, TX 77445*

Los Alamos
NATIONAL LABORATORY
Los Alamos, New Mexico 87545

PROBLEMS ENCOUNTERED DURING IMPACT CALCULATIONS USING ANALYTIC EQUATIONS OF STATE

by

Jerry F. Kerrisk and William B. Harvey

ABSTRACT

During modeling of the impact of a projectile on a target or other calculations that bring materials together at high velocities, computer simulations of materials being shocked to high pressure and then releasing to low pressure are performed. Depending on the circumstances, the release to low pressure is often accompanied by release to a very low density. Numerical problems leading to very large sound speeds (and thus small time steps) or to negative Lagrangian volumes have been encountered during MESA-2D calculations of this nature. These problems can be traced to the behavior of the equation of state (EOS) in the limit as the density becomes much less than the normal or reference density. Although analytic solutions for expansion isentropes may show acceptable behavior in the low-density limit, numerical solutions can show undesirable behavior. Examples of this undesirable behavior in the low-density regime are given for some simple, analytic equations of state that have closed-form solutions for isentropes. The behavior of three analytic EOSs that are frequently used in MESA-2D calculations are then discussed. These EOSs are the Los Alamos EOS, the MESA polynomial EOS, and a Mie-Grüneisen EOS based on a linear relation between shock and particle velocity. The problems in the low-density region can be corrected for the Los Alamos EOS and the MESA polynomial EOS by the proper choice of EOS coefficients in the expansion region (density less than the reference density). Problems with the Mie-Grüneisen EOS can be corrected if the functional relationship between the Grüneisen parameter (Γ) and density differs above and below the reference density.

INTRODUCTION

In MESA-2D calculations simulating the impact of materials or the penetration of a projectile into or through a target, high pressures are calculated in the materials by the modeling of shock processes and adiabatic compressions. Whenever free surfaces are modeled, the computation will follow materials releasing from high-pressure states to zero or nearly zero pressure. If the release proceeds to densities much lower than the normal density, numerical problems can be encountered in the simulations. The occurrence of these problems depends on the equation of state (EOS) of the material involved.

Two classes of problems have been encountered, very high material velocities that lead to advection difficulties and very small time steps that slow or stop a calculation. MESA-2D calculations use one or more Lagrangian steps followed by an advection step in which cells are returned to their original shape. Velocities are calculated at the vertices of cells. Large material velocities can lead to negative Lagrangian volumes, which stop the calculation. These velocities can be much larger than any realistic material velocity that could be expected in the calculation and often occur in a small region (a few cells) of the problem. An examination of the one or few cells with this condition usually indicates one or more materials with low density, large specific internal energy (positive or negative), and sometimes very large negative values of c^2, where c is the calculated bulk sound speed of the material in the cells. Calculations can also be slowed or even stopped if the time step becomes too small. Frequently, in such situations the time step will be controlled by a single calculational cell or a few cells that are contiguous. An examination of the cell or cells controlling the time step reveals conditions very similar to the case of negative Lagrangian volumes except that c^2 is very large and positive.

The numerical behavior of a calculation that encounters such problems can be very erratic. It is sometimes possible to stop and restart the calculation a short time before the occurrence of the problem with a different time step and pass over the time when the problem occurred. However, this technique will often only delay the occurrence of the problem. The same type of problem will stop the calculation a short time later in the same computational cell or a nearby cell. A more robust solution is to drop the offending material from the region where the problem occurs at a time before the material velocities, sound speeds, or energies have gotten out of hand. In either case these solutions can be costly in terms of the amount of time the user must spend to 'fix' the problem. Another solution in MESA-2D is to use the 'CLEAN' option. However, this option only drops low-density material in mixed cells, so that material in pure cells that exhibits these problems will still exist.

Experience has shown that problems of negative Lagrangian volumes and small time steps are intimately connected to the behavior of the EOS of a material. In particular, if the pressure (P) of the EOS does not approach zero as the density (ρ) goes to zero then the problems discussed above are frequently encountered. If the EOS is well behaved in the expansion region ($P \rightarrow 0$ as $\rho \rightarrow 0$), such problems rarely arise.

Any expansion process that is simulated in hydrodynamic calculations in which strength and viscosity effects are not modeled should occur isentropically. For a variety of reasons, such calculations do not always maintain the isentropic nature of the expansion process. Deviations from isentropic conditions can often be traced to the interplay of the EOS and the numerical schemes implemented in the hydrodynamic code. When the EOS is not well behaved in a given density region, the computational results can be catastrophic. For these reasons, it is important to understand the behavior of isentropes as determined by the EOS. It is also important to understand the behavior of an EOS as the differential equation defining an isentrope is integrated numerically. The time-step procedure used in hydrocode calculations is effectively a numerical-integration process. Although an EOS can show a well-behaved analytic isentrope in the low-density limit, numerical integration can lead to large deviations of the energy, pressure, or sound speed from realistic values.

In this report, a number of simple analytic EOSs are discussed initially. Although these EOSs are not often used for realistic calculations, they have closed-form analytic solutions for an isentrope and provide examples of good and bad behavior in the limit as density becomes much less than the normal density of the material. The behavior of three EOSs that are used in impact problems, the Los Alamos EOS, the MESA polynomial EOS, and a Mie-Grüneisen EOS based on a linear relation between shock and particle velocity, are then discussed. With these EOSs, unpredictable behavior can occur during an isentropic expansion to low density or in the calculation of the sound speed at low density. The purpose of this report is to investigate the behavior of these EOSs at low density and to propose solutions to the problems found.

EXPANSION ALONG AN ISENTROPE

Along an isentrope, changes in specific internal energy (ε) are related to changes in density (ρ) or specific volume ($V = 1/\rho$) by the equation

$$d\varepsilon = -P\,dV = (P/\rho^2)\,d\rho\ , \qquad (1)$$

where P is the pressure defined by the EOS as a function of ρ and ε. Clearly, a numerical integration of Eq. (1) along a path as the density approaches zero will eventually cease to be meaningful unless the EOS is well behaved and $P \rightarrow 0$ as $\rho \rightarrow 0$ along an isentrope. Even if the EOS is well behaved, the numerical integration scheme inherent in hydrocode calculations may have problems. The behavior of $(\partial P/\partial \varepsilon)_\rho$, which influences the stability of a numerical integration scheme for Eq. (1), is also of interest in the limit as $\rho \rightarrow 0$ (Gear 1971).

If Eq. (1) has a closed-form analytic solution for a particular EOS, the behavior of isentropes at low density can be understood from this solution. A number of simple EOSs that have closed-form analytic solutions for Eq. (1) are discussed below. The problem with hydrocode calculations is that analytic solutions to Eq. (1) are not used. Material energy changes in each cell are calculated from the PV work done during a time step. This process is effectively a numerical integration of Eq. (1). Thus, the numerical behavior of Eq. (1) is also important for understanding the problems discussed above.

SOUND SPEED

In a hydrodynamic code, an important consideration is the calculation of the time step, δt. One simple method uses the bulk sound speed of a material, c, and the size of a computational cell, δh, in the equation

$$\delta t \leq \delta h / c\ . \qquad (2)$$

Equation (2) is frequently referred to as the Courant condition, and for a Lagrangian calculation it simply states that the time step should not be larger than the time required for a wave to cross a computational cell.

From thermodynamic considerations, the bulk sound speed of a material is calculated as

$$c^2 = (\partial P/\partial \rho)_S \ , \qquad (3)$$

where S is the specific entropy. For an EOS where P is given as a function of ε and ρ, c^2 is calculated as

$$c^2 = (\partial P/\partial \rho)_\varepsilon + (P/\rho^2)\,(\partial P/\partial \varepsilon)_\rho \ . \qquad (4)$$

Unless P or $(\partial P/\partial \varepsilon)_\rho$ or both approach zero as $\rho \rightarrow 0$ for an EOS, the second term in Eq. (4) can lead to problems with large sound speeds and thus small time steps. In hydrodynamic calculations, the bulk sound speed can exhibit a wide range of behavior. In the limit as $\rho \rightarrow 0$, c^2 may become very large, go to zero or asymptote to a finite value. In some cases, negative values of c^2 may be calculated. MESA-2D ignores negative values of c^2 (sets negative c^2 to zero), but they are an indication of possible problems.

NUMERICAL METHODS

As noted above, hydrocodes perform numerical integrations of systems of differential equations. To assess the numerical performance of the various EOSs discussed here, two numerical integration schemes were used to integrate Eq. (1) along expansion isentropes. The first was a simple Euler method (Gear 1971) in which the energy was advanced from step i to step i+1 as

$$\varepsilon_{i+1} = \varepsilon_i + (P_i / \rho_i^2)\,(\rho_{i+1} - \rho_i) \ , \qquad (5)$$

where $\rho_{i+1} = f\,\rho_i$. The value of f was taken as 0.95. This explicit method keeps the change in density scaled to the size of the density as it approaches zero. The results were not significantly affected by the value of f. EOSs that exhibited numerical difficulties showed the same difficulties for larger or smaller step sizes in density. The density at which the difficulties began was a weak function of f.

The second numerical integration scheme was an Adams-Bashforth-Moulton predictor-corrector (ABM-PC) method of variable order (1-12) (Gear 1971, Shampine and Watts 1979). This method is recommended for non-stiff and mildly stiff differential equations. A relative error tolerance of 3×10^{-5} was used. The implementation employed stops if the differential equation appears to be too stiff to achieve the required error tolerance.

SIMPLE ANALYTIC EOSs

This section discusses three simple analytic EOSs that have analytic solutions for isentropes in P-ρ space and ε-ρ space. Although these EOSs are not often used to describe solid materials in realistic impact problems, their simplicity is useful for illustrating the behavior of release isentropes at very low densities.

Ideal Gas

The first EOS to be considered is an ideal-gas form given by the equation

$$P = (\gamma - 1)\,\rho\,\varepsilon \ , \qquad (6)$$

where γ is a constant such that $\gamma > 1$. Equation (6) can be directly substituted into Eq. (1) and integrated to give

$$\varepsilon = \varepsilon_r (\rho / \rho_r)^{\gamma-1} , \tag{7}$$

where ε_r and ρ_r are values of specific internal energy and density at some reference point along the isentrope. By substituting Eq. (7) for ε into Eq. (6), the variation of pressure along an isentrope is given by

$$P = P_r (\rho / \rho_r)^{\gamma} , \tag{8}$$

where P_r and ρ_r are the values of pressure and density at some reference point along the isentrope. From Eqs. (4) and (6), the behavior of the sound speed of an ideal gas is

$$c^2 = \gamma P/\rho = \gamma(\gamma-1)\varepsilon . \tag{9}$$

Equation (9) holds in general; along an isentrope the sound speed can be related to density as

$$c = c_r (\rho / \rho_r)^{(\gamma-1)/2} , \tag{10}$$

where c_r and ρ_r are the values of sound speed and density at some reference point along the isentrope. Since γ is greater than one, Eqs. (7), (8), and (10) clearly show that the specific internal energy, pressure, and bulk sound speed all approach zero as the density approaches zero along an isentrope. Equation (6) also shows that, in general, the pressure approaches zero as the density approaches zero as long as the specific internal energy remains finite. Numerical solutions of ideal gas isentropes are also well behaved in the limit as $\rho \rightarrow 0$.

Stiffened Gas EOS

In the stiffened gas EOS (Harlow and Amsden 1971), the pressure is defined as

$$P = (\gamma-1)\rho\varepsilon + \mathbf{a}(\rho-\rho_0) , \tag{11}$$

where γ is again a constant such that $\gamma > 1$, $\mathbf{a}$ is a positive constant, and ρ_0 is the normal or initial density of the material. The first term in Eq. (11) is the ideal-gas form. Equation (11) is a form of a Mie-Grüneisen EOS. It can also be considered as a kind of first-order expansion of a gas EOS around ρ_0 except that $\mathbf{a}$ need not be small. In fact, for a solid, $\mathbf{a}$ equals the square of the sound speed ($\mathbf{a} = c_0^2$) at ambient conditions ($\varepsilon = 0$ and $\rho = \rho_0$).

In the limit as $\rho \rightarrow 0$, Eq. (11) indicates that the pressure approaches a value independent of ρ and ε, $P \rightarrow -\mathbf{a}\rho_0$ and that $(\partial P/\partial\varepsilon)_\rho \rightarrow 0$. However, the behavior of ε must be examined in greater detail to determine the behavior of P along an isentrope. Substituting Eq. (11) into Eq. (1) and integrating gives a relation between ε and ρ along an isentrope as

$$\varepsilon = K(\rho/\rho_0)^{(\gamma-1)} - \mathbf{a}\{[1/(\gamma-1)] - (\rho_0/\rho\gamma)\}, \qquad (12)$$

where K is a constant along a given isentrope but does depend on the entropy and thus varies from one isentrope to another. Substituting Eq. (12) into Eq. (11) gives the pressure along an isentrope as

$$P = K\rho_0(\gamma-1)(\rho/\rho_0)^{\gamma} - \mathbf{a}\rho_0/\gamma . \qquad (13)$$

From Eq. (12) it is evident that $\varepsilon \rightarrow \infty$ in the limit as $\rho \rightarrow 0$ and from Eq. (13) that $P \rightarrow -\mathbf{a}\rho_0/\gamma$ as $\rho \rightarrow 0$ along all isentropes. The terms in Eqs. (12) and (13) that dominate for $\rho << \rho_0$ are independent of K (independent of the initial entropy). Thus, all isentropes collapse to the same curve in this limit for this EOS.

From Eqs. (4) and (11), the sound speed of the stiffened gas EOS is given by

$$c^2 = \gamma(\gamma-1)\varepsilon + \mathbf{a}\{\gamma - [(\gamma-1)\rho_0/\rho]\} . \qquad (14)$$

At first glance at Eq. (14), it would appear that $c^2 \rightarrow -\infty$ as $\rho \rightarrow 0$. However, this is not the case along an isentrope when the behavior of ε is taken into account. When Eq. (12) is substituted into Eq. (14), the variation of c^2 along an isentrope is given by

$$c^2 = \gamma(\gamma-1)K(\rho/\rho_0)^{(\gamma-1)} , \qquad (15)$$

which is the same as an ideal gas EOS. Thus, $c^2 \rightarrow 0$ as $\rho \rightarrow 0$ along an isentrope. The form of Eq. (15) results from cancellation of terms that become large and positive, and large and negative as $\rho \rightarrow 0$. Thus, a calculation of c^2 from Eq. (14), as is done in a hydrocode, can lead to difficulties even though an isentropic process is involved because the large positive and negative terms may not cancel exactly.

As an example of the numerical behavior of this EOS, constants that approximate the EOS of Al were chosen. Appendix A lists the values of $\mathbf{a}$ and ρ_0 used. Figures 1 - 3 show plots of the energy, pressure, and sound speed along an isentrope through a point on the Hugoniot at P = 10 Mbar (ρ = 5.949 g/cm^3, and ε = 1.011 Mbar-cm^3/g). In each plot three curves are shown, the analytic relation given by Eqs. (12), (13), or (15), and two numerical solutions to Eq. (1) for this EOS. The numerical solutions calculate ε as a function of ρ along the isotherm from Eq. (1). The values of ε and ρ on the isotherm are used to calculate the pressure from Eq. (11) and the sound speed from Eq. (14).

The large increase in ε as $\rho \rightarrow 0$ is evident for all three solutions in Fig. 1. The pressure (Fig. 2) approaches the value $-\mathbf{a}\rho_0/\gamma$ as $\rho \rightarrow 0$; however, in the case of the Euler solution the result at low density differs noticeably from the analytic solution. The sound speed (Fig. 3) approaches zero as $\rho \rightarrow 0$ for the analytic solution. However, the two numerical solutions deviate significantly from the analytic solution at low density. The sound speed from the Euler solution is quite inaccurate for densities below ~1 g/cm^3, and $c^2 \rightarrow -\infty$ as $\rho \rightarrow 0$. The sound speed from the ABM-PC solution follows the analytic solution to lower densities but eventually drifts

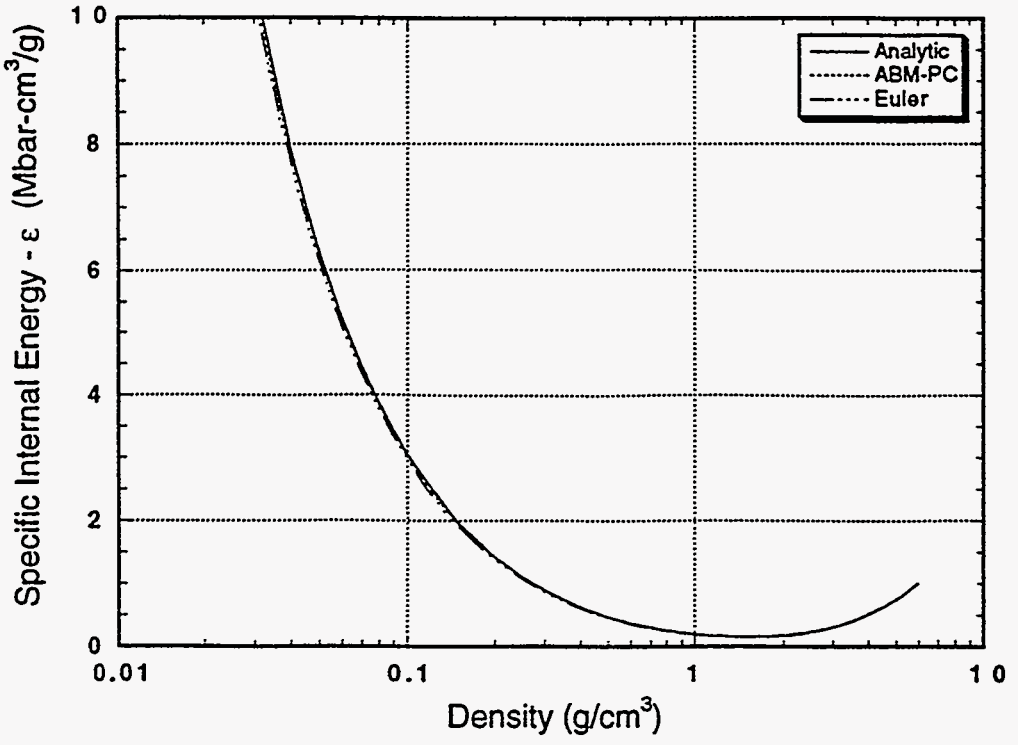

Fig. 1. Specific internal energy (ε) as a function of density (ρ) along an isentrope through 10 Mbar on the Hugoniot for a stiffened gas EOS for Al.

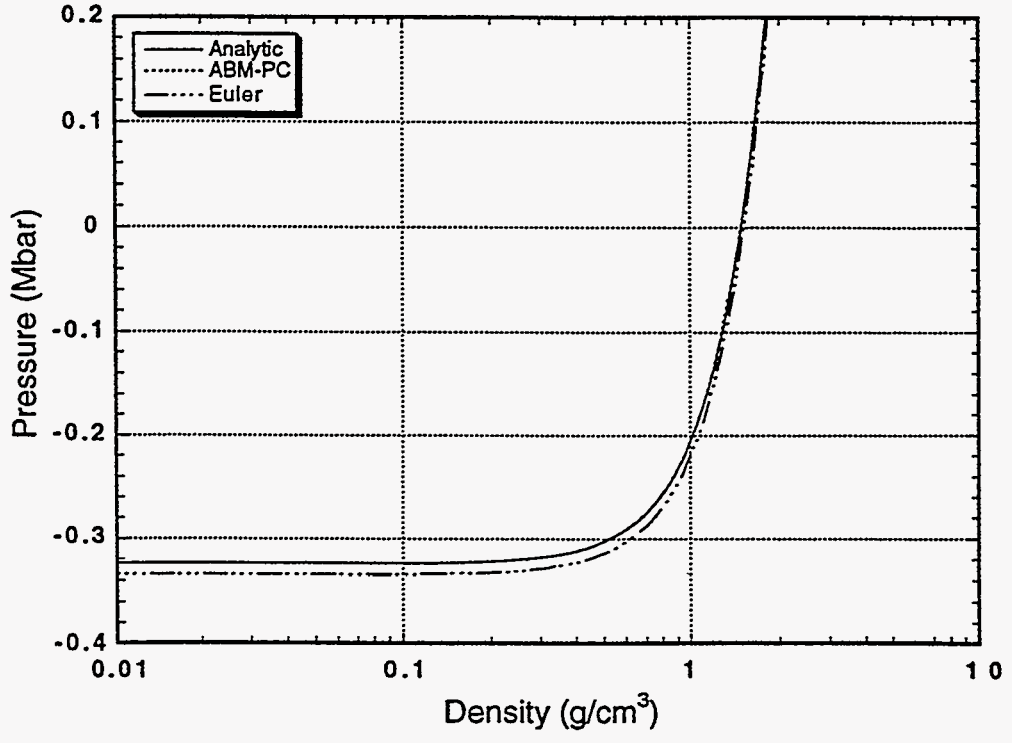

Fig. 2. Pressure (P) as a function of density (ρ) along an isentrope through 10 Mbar on the Hugoniot for a stiffened gas EOS for Al.

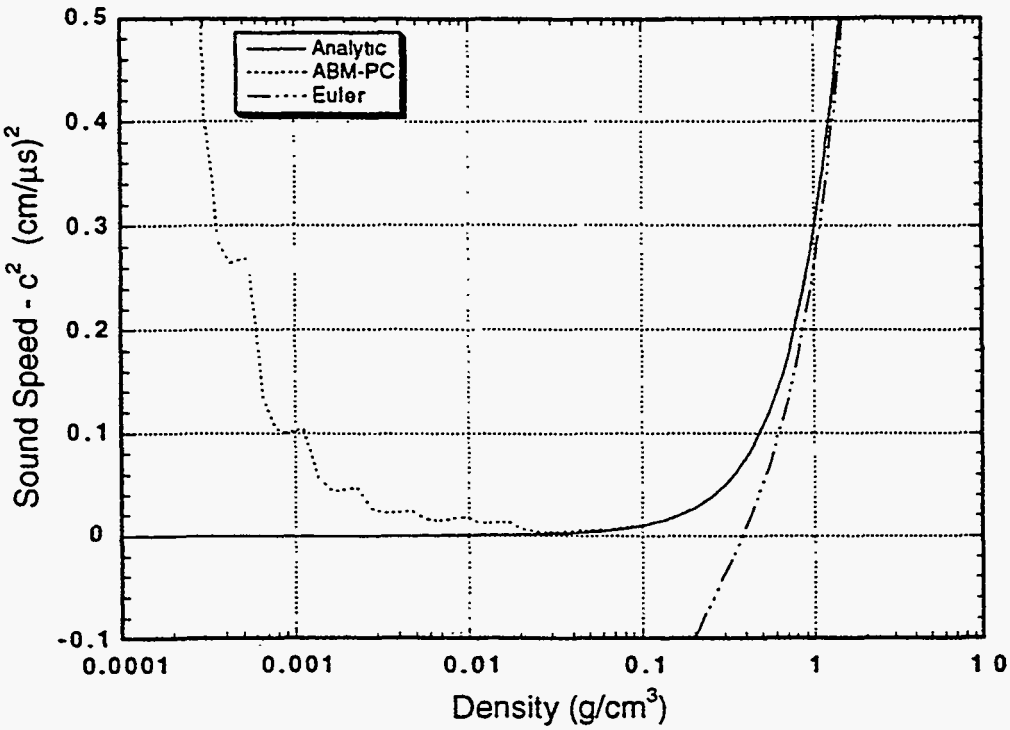

Fig. 3. Sound speed (c^2) as a function of density (ρ) along an isentrope through 10 Mbar on the Hugoniot for a stiffened gas EOS for Al.

away. The sound speeds from both numerical schemes become inaccurate because they do not get complete cancellation of the terms that cancel analytically. The exact manner in which c^2 deviates from the zero limit as $\rho \rightarrow 0$ depends on the form of the numerical solution.

Modified Stiffened Gas EOS

Equation (11) can be modified to eliminate the catastrophic behavior of ε along an isentrope by defining pressure as

$$P = (b_0 \rho_0 + b_1 \rho)\,\varepsilon + \mathbf{a}\,(\rho - \rho_0)\ , \qquad (16)$$

where $\mathbf{a}$, b_0, and b_1 are positive constants. Compared to Eq. (11), a term that is independent of density and linear in ε has been added.

In the limit as $\rho \rightarrow 0$, Eq. (16) indicates that the pressure approaches a value dependent on ε, $P \rightarrow -\mathbf{a}\,\rho_0 + b_0\,\rho_0\,\varepsilon$ and that $(\partial P/\partial \varepsilon)_\rho \rightarrow b_0\,\rho_0$. As with the stiffened gas EOS, however, behavior along an isentrope needs to be examined. Substituting Eq. (16) for pressure into Eq. (1) gives a differential equation that has analytic solutions for cases where b_1 is an integer. Although this is a limitation for a realistic description of a material, for the purposes of illustrating problems of EOSs at low density it is an acceptable limitation. With the restriction that $b_1 = 1$, the isentrope is given by

$$\varepsilon = (\mathbf{a} / b_0)\,[1 - (\rho / \rho_0) - (\rho / \rho_0\, b_0)\,] + K\,(\rho / \rho_0)\,\exp(-b_0\,\rho_0 / \rho)\ , \qquad (17)$$

where K is a constant that depends only on the entropy of the material along the isentrope. Substituting Eq. (17) into Eq. (16) gives a relation for the pressure along an isentrope as

$$P = [\,(\mathbf{a}\,\rho_0 / b_0)\,(\rho / \rho_0)^2\,(1 + 1/b_0)\,] + K\,[b_0 + (\rho / \rho_0)]\,\rho\,\exp(-b_0\,\rho_0 / \rho)\ . \qquad (18)$$

In the limit as $\rho \rightarrow 0$, Eq. (17) indicates that $\varepsilon \rightarrow (\mathbf{a} / b_0)$ and Eq. (18) that $P \rightarrow 0$ along all isentropes. For this EOS also, all isentropes collapse to the same curve for $\rho << \rho_0$.

From Eqs. (4) and (16), the sound speed of the modified stiffened gas is given by

$$c^2 = \{\,1 + [\,1 + (b_0\,\rho_0 / \rho)\,]^2\,\}\,\varepsilon + \mathbf{a}\,\{\,1 + [1 - (\rho_0 / \rho)\,][\,1 + (b_0\,\rho_0 / \rho)\,]\,\}\ . \qquad (19)$$

Equation (19) indicates that in general, c^2 can become infinite as $\rho \rightarrow 0$. However, when the behavior of ε along an isentrope (Eq. (17)) is taken into account, the sound speed along an isentrope is given by

$$c^2 = K\,\{\,1 + [\,1 + (b_0\,\rho_0 / \rho)\,]^2\,\}\,(\rho / \rho_0)\,\exp(-b_0\,\rho_0 / \rho) - \{\,(2\,\mathbf{a} / b_0)\,(\rho / \rho_0)\,(1 + 1/b_0)\,\}\ . \qquad (20)$$

From Eq. (20), $c^2 \rightarrow 0$ as $\rho \rightarrow 0$ along an isentrope.

As an example of the numerical behavior of this EOS, constants that approximate the EOS of Al were chosen. Appendix A lists the values of $\mathbf{a}$, b_0, b_1, and ρ_0 used. Figures 4 - 6 show plots of the energy, pressure, and sound speed along an isentrope through a point on the Hugoniot at P = 10 Mbar (ρ = 5.556 g/cm^3, and ε = 0.952 Mbar-cm^3/g). In each plot three curves are shown: the analytic relation given by Eqs. (17), (18), or (20), and two numerical solutions to Eq. (1) for this EOS. The numerical solutions calculate ε as a function of ρ along the isotherm from Eq. (1). The values of ε and ρ on the isotherm are used to calculate the pressure from Eq. (16) and the sound speed from Eq. (19).

The value of ε approaches 0.2 Mbar-cm^3/g as $\rho \rightarrow 0$ for the analytic solution and for the ABM-PC solution. However, the ABM-PC solution stopped at a density of ~0.01 g/cm^3 because of the large number of steps needed to achieve the requested relative accuracy. At this density the ABM-PC method was using a density step size of ~4x10^{-5} g/cm^3. If an attempt is made to push the ABM-PC method to lower densities by relaxing the error tolerance, large fluctuations in energy are ultimately encountered. The Euler solution becomes unstable at a density of ~0.02 g/cm^3, leading to large fluctuations in the energy. The pressure (Fig. 5) approaches zero as $\rho \rightarrow 0$ for the analytic solution and the ABM-PC solution; however, the ABM-PC solution for the pressure shows small fluctuations below a density of ~0.03 g/cm^3. The Euler solution for the pressure shows large fluctuations at a density of ~0.02 g/cm^3 because it is based on the energy. The sound speed (Fig. 6)

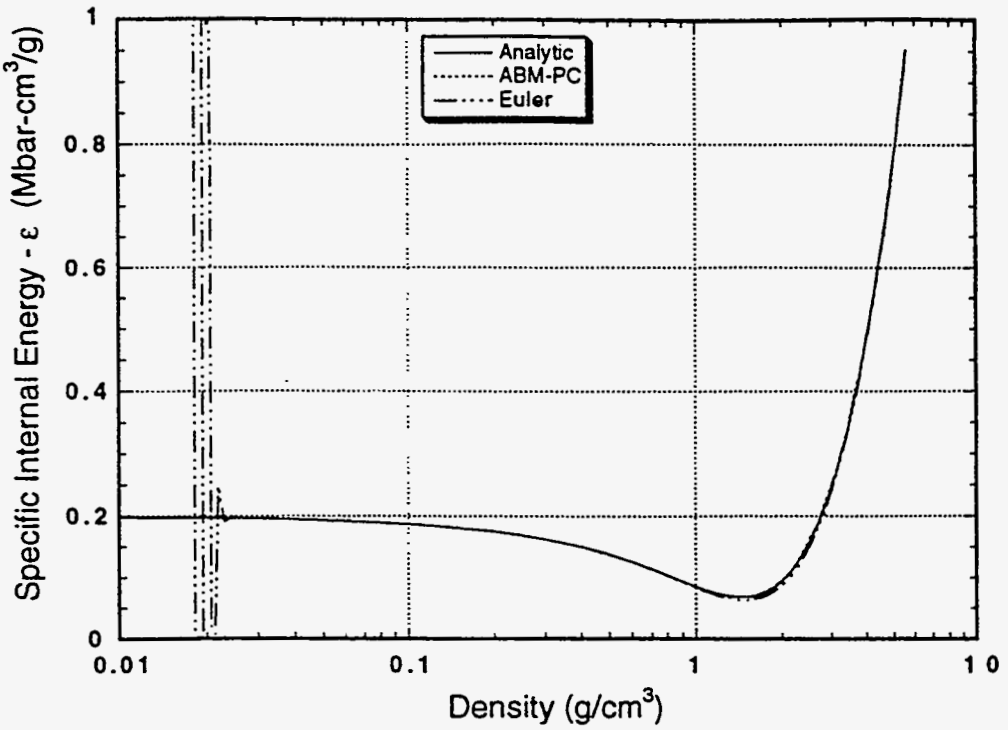

Fig. 4. Specific internal energy (ε) as a function of density (ρ) along an isentrope through 10 Mbar on the Hugoniot for a modified stiffened gas EOS for Al.

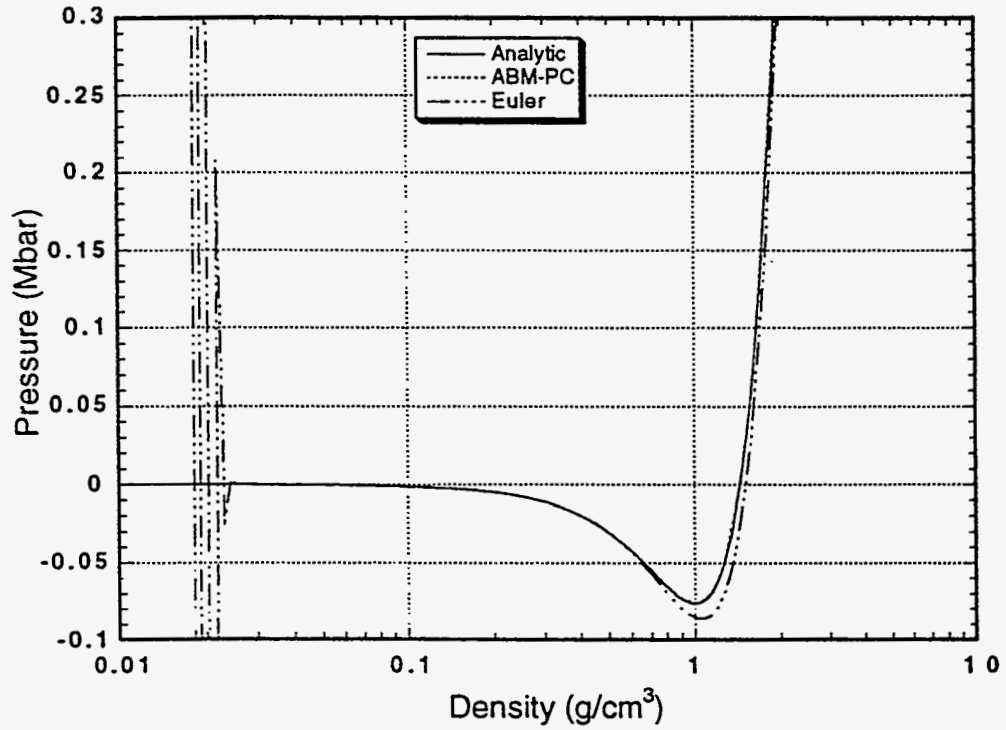

Fig. 5. Pressure (P) as a function of density (ρ) along an isentrope through 10 Mbar on the Hugoniot for a modified stiffened gas EOS for Al.

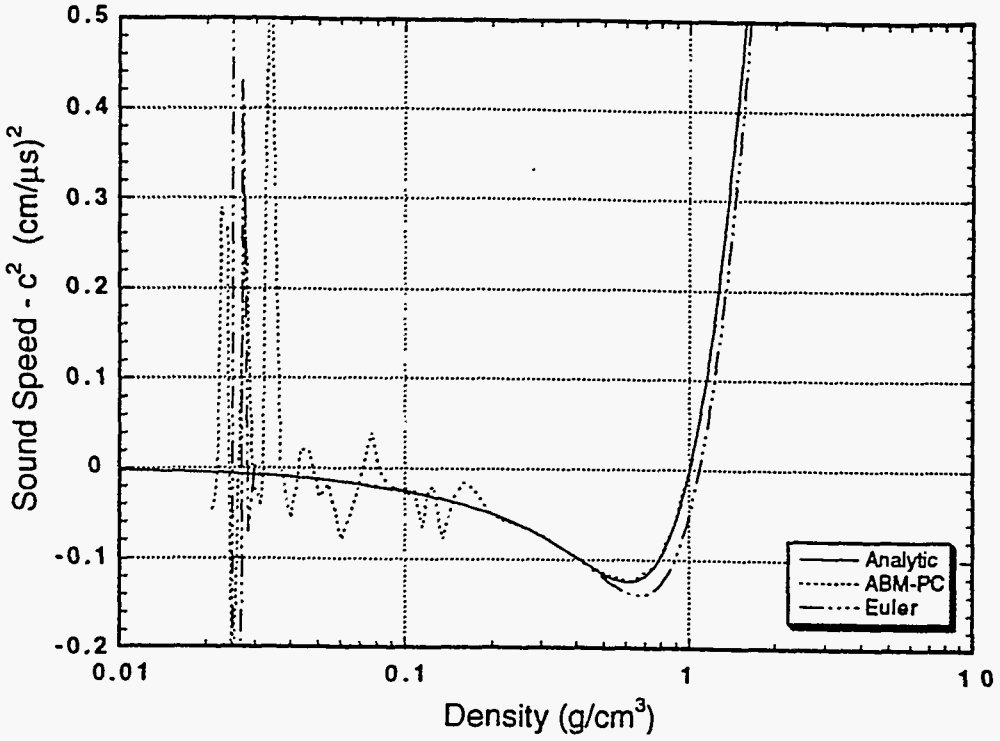

Fig. 6. Sound speed (c^2) as a function of density (ρ) along an isentrope through 10 Mbar on the Hugoniot for a modified stiffened gas EOS for Al.

approaches zero for the analytic solution. For the ABM-PC solution, c^2 begins to show fluctuations below a density of ~0.2 g/cm^3, the fluctuations becoming large by a density of 0.03 g/cm^3. For the Euler solution, large fluctuations in c^2 begin at about the same density as those for the energy and pressure. Although the analytic forms of isentropes of this EOS appear to show acceptable behavior, the numerical solutions developed numerical difficulties at sufficiently low densities.

LOS ALAMOS EOS

The Los Alamos EOS that is used in MESA-2D defines P as a function of ε and ρ as

$$P = [\, A_o(\mu) + B_o(\mu)\,(\varepsilon\,\rho_0) + C_o(\mu)\,(\varepsilon\,\rho_0)^2\,]\,/\,Q\,, \tag{21}$$

where

$$A_o(\mu) = a_0 + a_1\,\mu + a_2^*\,\mu^2\,, \tag{22a}$$

$$B_o(\mu) = b_0 + b_1\,\mu + b_2^*\,\mu^2\,, \tag{22b}$$

$$C_o(\mu) = c_0 + c_1\,\mu + c_2^*\,\mu^2\,, \tag{22c}$$

$$Q = \varepsilon\,\rho_0 + \varepsilon_0\,, \tag{22d}$$

and $\mu = (\rho/\rho_0) - 1$. This form differs somewhat from the original formulation in the treatment of the terms that are quadratic in μ. (Zukas et al. 1982). The quantities a_i, b_i, c_i, and ε_0 are constants, and ρ_0 is the normal density of the material. The constant a_0 is normally zero and will be assumed so in subsequent discussions. The constants a_2^*, b_2^*, and c_2^* differ depending on whether μ is positive or negative (ρ is greater than or less than ρ_0). For $\mu > 0$, $a_2^* = a_2^c$, $b_2^* = b_2^c$, and $c_2^* = c_2^c$, where the superscript c indicates that the material is in compression. For $\mu < 0$, $a_2^* = a_2^e$, $b_2^* = b_2^e$, and $c_2^* = c_2^e$, where the superscript e indicates that the material is expanded relative to the initial state. Thus, the user has the freedom to choose all six coefficients independently.

The sound speed of the Los Alamos EOS is calculated from Eqs. (4) and (21) as

$$c^2 = \{ [A^\dagger_o(\mu) + B^\dagger_o(\mu)(\varepsilon \rho_0) + C^\dagger_o(\mu)(\varepsilon \rho_0)^2] / (\rho_0 Q) \} + \{ P [\rho_0 B_0(\mu) + 2 \rho_0^2 \varepsilon C_0(\mu)] / (Q \rho^2) \} - \{ (P^2 \rho_0) / (Q \rho^2) \} , \quad (23)$$

where

$$A^\dagger_o(\mu) = a_1 + 2 a_2^* \mu , \quad (24a)$$

$$B^\dagger_o(\mu) = b_1 + 2 b_2^* \mu , \text{ and} \quad (24b)$$

$$C^\dagger_o(\mu) = c_1 + 2 c_2^* \mu . \quad (24c)$$

This EOS does not have an analytic solution for an isentrope. However, it is possible to obtain an analytic solution in the limit for $\rho << \rho_0$. That solution provides some insight into the behavior of the Los Alamos EOS.

Behavior in the Low-Density Limit

The behavior of the pressure in Eq. (21) as $\rho \rightarrow 0$ can be written as

$$P = [A'' + A' (\rho/\rho_0) + B'' (\rho_0 \varepsilon) + B' (\rho_0 \varepsilon)(\rho/\rho_0) + C'' (\rho_0 \varepsilon)^2 + C' (\rho_0 \varepsilon)^2 (\rho/\rho_0)] / Q \quad (25)$$

where

$$A'' = -a_1 + a_2^e , \quad (26a)$$

$$A' = a_1 - 2 a_2^e , \quad (26b)$$

$$B'' = b_0 - b_1 + b_2^e , \quad (26c)$$

$$B' = b_1 - 2 b_2^e , \quad (26d)$$

$$C'' = c_0 - c_1 + c_2^e , \quad (26e)$$

$$C' = c_1 - 2 c_2^e . \quad (26f)$$

Unless A", B", and C" are identically zero, P will not, in general, approach zero as $\rho \rightarrow 0$.

As with the simpler EOSs discussed above, the behavior of ε and P along an expansion isentrope is more significant than the general behavior. An analytic solution of Eq. (1) can be obtained in the limit of $\rho << \rho_0$ using the definition of the pressure given in Eq. (25). In this limit and assuming that A", B", and C" are not zero, the energy and density along an isentrope are related as

$$-1/\rho = \{ [\varepsilon_0 - (B"/2C")] / W \} \ln[(2C" \rho_0^2 \varepsilon + B" \rho_0 - W) / (2C" \rho_0^2 \varepsilon + B" \rho_0 + W)] + [1 / (2 C" \rho_0)] \ln[A" + B" \rho_0 \varepsilon + C"(\rho_0 \varepsilon)^2] + K \quad (27)$$

where

$$W^2 = \rho_0^2 [B"^2 - 4 A" C"] , \quad (28)$$

and K is a constant along a given isentrope. In the limit as $\rho \rightarrow 0$, the left-hand side (LHS) of Eq. (27) approaches $-\infty$. The right-hand side (RHS) of Eq. (27) will approach $-\infty$ if the arguments of the 'ln' terms approach zero as $\rho \rightarrow 0$. In this limit, the energy can approach either of two values

$$\varepsilon = (W - B" \rho_0) / (2 C" \rho_0^2) , \quad (29a)$$

or

$$\varepsilon = (-W - B" \rho_0) / (2 C" \rho_0^2) . \quad (29b)$$

If the Los Alamos EOS coefficients are chosen such that A", B", and C" are zero, the analytic solution to Eq. (1) in the limit of $\rho << \rho_0$ becomes

$$(\rho/\rho_0) = K [(2C'\rho_0^2 \varepsilon + B' \rho_0 - W) / (2C' \rho_0^2 \varepsilon + B' \rho_0 + W)]^m [A' + B' \rho_0 \varepsilon + C'(\rho_0 \varepsilon)^2]^n , \quad (30)$$

where

$$m = \rho_0 \{ [\varepsilon_0 - (B'/2C')] / W \} , \quad (31a)$$

and

$$n = 1 / (2 C') . \quad (31b)$$

As $\rho \rightarrow 0$, the LHS of Eq. (30) also approaches zero. The RHS will approach zero (for m and n positive) if the energy approaches the values

$$\varepsilon = (W - B' \rho_0) / (2 C' \rho_0^2) , \quad (32a)$$

or

$$\varepsilon = (-W - B' \rho_0) / (2 C' \rho_0^2) . \quad (32b)$$

This analysis indicates that as $\rho \rightarrow 0$ along an isentrope, ε approaches a nonzero value whether the coefficients are chosen so that A", B", and C" are zero or nonzero. This behavior is analogous to that of the modified stiffened gas EOS. Because of the complex relation between ε and ρ along an isentrope, even for $\rho << \rho_0$, it was not possible to obtain analytic expressions for P or c^2 along an isentrope in that limit. For their behavior it will be necessary to examine numerical solutions to Eq. (1).

Numerical Expansion Isentropes

To perform numerical integrations of Eq. (1) it will be necessary to choose values of the coefficients a_i, b_i, and c_i. The normal choice of the expansion coefficients is

$$a_2^e = -a_2^c , \tag{33a}$$

$$b_2^e = b_2^c , \text{ and} \tag{33b}$$

$$c_2^e = 0. \tag{33c}$$

For this choice, A", B", and C" are not zero, and the pressure and $(\partial P/\partial \varepsilon)_\rho$ do not approach zero in general as $\rho \rightarrow 0$. The pressure calculated by the Los Alamos EOS can be forced to zero as $\rho \rightarrow 0$ by requiring that the coefficients a_2^e, b_2^e, and c_2^e are related to the other coefficients as

$$a_2^e = a_1 , \tag{34a}$$

$$b_2^e = b_1 - b_0 , \text{ and} \tag{34b}$$

$$c_2^e = c_1 - c_0 . \tag{34c}$$

This choice makes A", B", and C" identically zero. The use of Eqs. (34) forces P and $(\partial P/\partial e)_\rho$ to zero as $\rho \rightarrow 0$. These definitions are not unreasonable. In general, the lack of experimental data in the expansion region ($\rho < \rho_0$) precludes experimental determination of the coefficients. Appendix A contains two sets of coefficients for Al for the Los Alamos EOS, one set with expansion coefficients defined by Eqs. (33) and the other with expansion coefficients defined by Eqs. (34).

Figures 7 - 9 show plots of energy, pressure, and sound speed as a function of density along an expansion isentrope through a point on the Hugoniot at P = 10 Mbar (ρ = 7.371 g/cm^3 and ε = 1.1722 Mbar-cm^3/g). The four curves in each plot show results from the Euler and ABM-PC methods using coefficient sets defined by Eqs. (33) and (34). For energy (Fig. 7), the Euler integration using the Eq. (33) coefficients experiences large fluctuations starting at a density of ~0.02 g/cm^3. The ABM-PC integration using these coefficients stopped at a density of ~0.005 g/cm^3 with an indication that the differential equation became too stiff to continue. If an attempt is made to push the ABM-PC method to lower densities by relaxing the error tolerance, large fluctuations in energy are ultimately encountered. When the Eq. (34) coefficients were used, the Euler and ABM-PC integrations continued to a density of ~1.0x10^{-9} g/cm^3 without apparent problems. The behavior of the pressure (Fig. (8)) is similar to that of the energy. The sound speed calculated

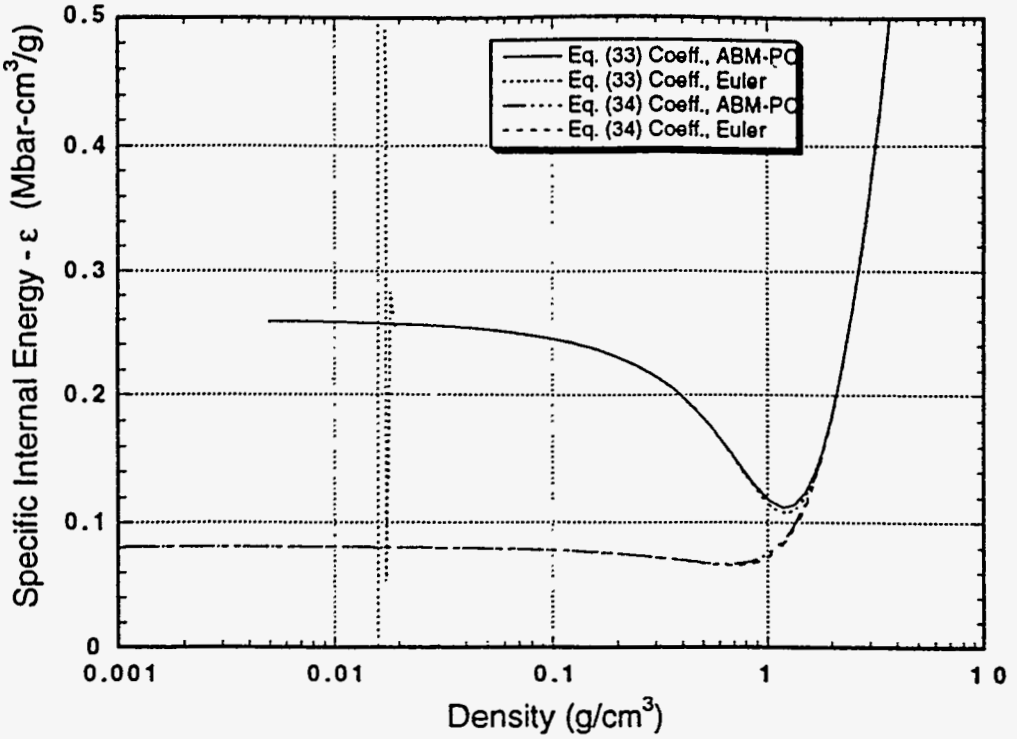

Fig. 7. Specific internal energy (ε) as a function of density (ρ) along an isentrope through 10 Mbar on the Hugoniot for a Los Alamos EOS for Al.

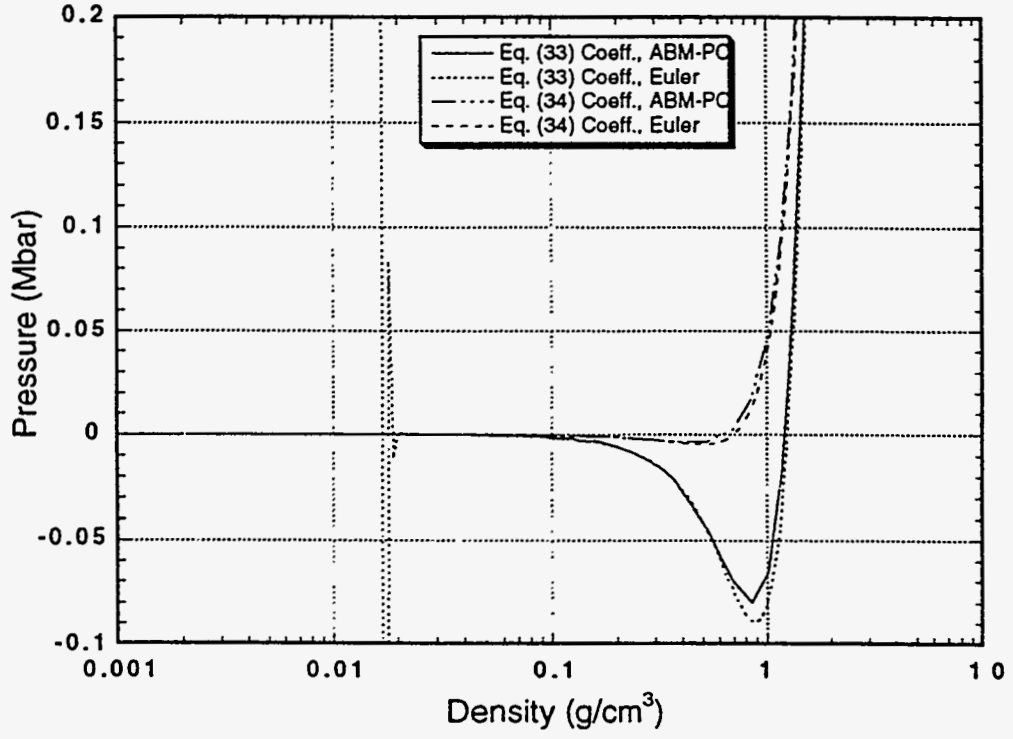

Fig. 8. Pressure (P) as a function of density (ρ) along an isentrope through 10 Mbar on the Hugoniot for a Los Alamos EOS for Al.

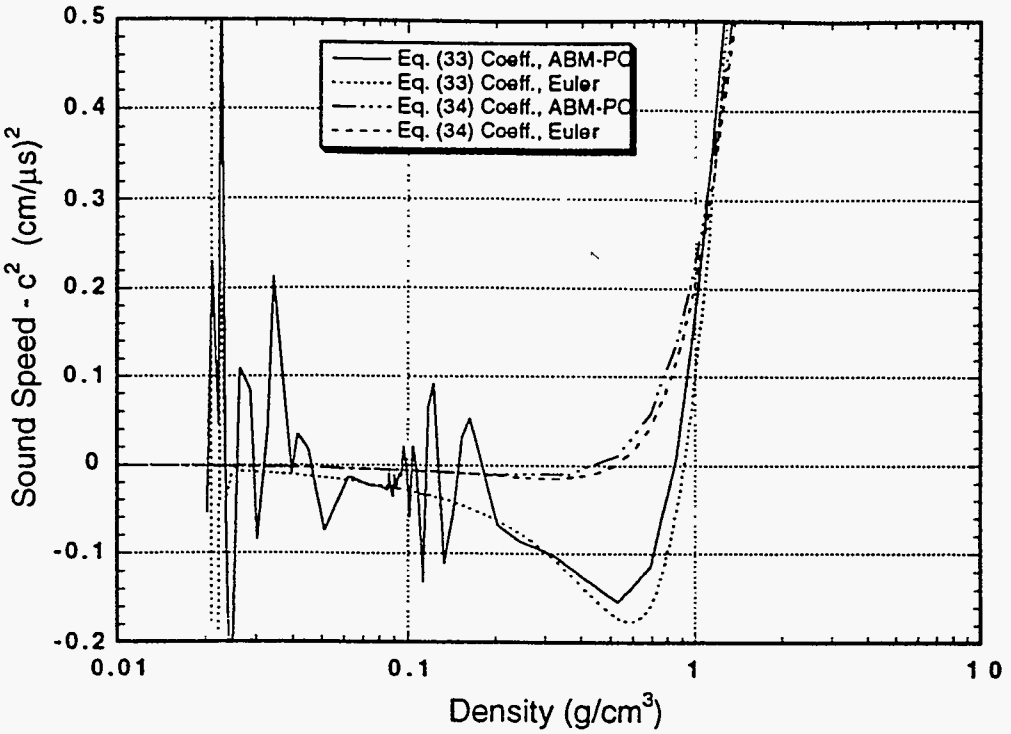

Fig. 9. Sound speed (c^2) as a function of density (ρ) along an isentrope through 10 Mbar on the Hugoniot for a Los Alamos EOS for Al.

with the Eq. (33) coefficients using the ABM-PC integration shows fluctuations starting at a density of ~0.2 g/cm^3; these fluctuations become large at a density of ~0.02 g/cm^3, the same density at which large fluctuations in the sound speed calculated by the Euler method begin. Sound speeds calculated with the Eq. (34) coefficients are negative but well behaved to densities of ~1.0x10^{-9} g/cm^3.

The two ways of defining coefficients in the expansion region lead to significantly different behavior of ε, P, and c^2 at densities below ρ_0. The energy (Fig. 7) asymptotes to very different values for the two sets of coefficients. The minimum pressure (Fig. 8) with the Eq. (33) definition is about –0.09 Mbar but with the Eq. (34) definition is only about –0.003 Mbar. Similarly, minimum values of c^2 (Fig. 9) are quite different. A comparison of the results for this isentrope using the Eq. (34) coefficients with tabular EOS data (Holian 1984) for Al is given in Appendix B.

POLYNOMIAL EOS

The polynomial EOS defines P as a function of ε and ρ as

$$P = A_p(\mu) + B_p(\mu)\,(\varepsilon\,\rho_0) \tag{35}$$

where

$$A_p(\mu) = a_0 + a_1 \mu + a_2^{\bullet} \mu^2 + a_3 \mu^3 \text{ , and} \qquad (36a)$$

$$B_p(\mu) = b_0 + b_1 \mu + b_2^{\bullet} \mu^2 + b_3 \mu^3 \text{ .} \qquad (36b)$$

The quantities a_i and b_i are constants. The constant a_0 is normally zero and will be assumed so in subsequent discussions. As with the Los Alamos EOS, the constants $a_2^{\bullet}$, and $b_2^{\bullet}$ differ depending on whether μ is positive or negative (ρ is greater than or less than ρ_0). In MESA-2D, for $\mu > 0$, $a_2^{\bullet} = a_2^c$ and $b_2^{\bullet} = b_2^c$; and for $\mu < 0$, $a_2^{\bullet} = a_2^e$ and $b_2^{\bullet} = b_2^e$. These four coefficients can be chosen independently.

The sound speed of the polynomial EOS can be calculated from Eq. (3) as

$$c^2 = \{ [A^{\dagger}_p(\mu) + B^{\dagger}_p(\mu) (\varepsilon \rho_0)] / (\rho_0) \} + (P/\rho^2) (B_p(\mu) \rho_0) \text{ ,} \qquad (37)$$

where

$$A^{\dagger}_p(\mu) = a_1 + 2a_2^{\bullet} \mu + 3a_3 \mu^2 \text{ , and} \qquad (38a)$$

$$B^{\dagger}_p(\mu) = b_1 + 2b_2^{\bullet} \mu + 3b_3 \mu^2 \text{ .} \qquad (38b)$$

As with the Los Alamos EOS, the polynomial EOS does not have an analytic solution for an isentrope. It is possible here, also, to obtain an analytic solution in the limit for $\rho << \rho_0$.

Behavior in the Low-Density Limit

The behavior of the pressure in Eq. (35) as $\rho \rightarrow 0$ can be written as

$$P = A_p'' + A_p' (\rho / \rho_0) + B_p'' (\rho_0 \varepsilon) + B_p' (\rho / \rho_0) (\rho_0 \varepsilon) \text{ ,} \qquad (39)$$

where

$$A_p'' = -a_1 + a_2^e - a_3 \text{ ,} \qquad (40a)$$

$$A_p' = a_1 - 2a_2^e + 3a_3 \text{ ,} \qquad (40b)$$

$$B_p'' = b_0 - b_1 + b_2^e - b_3 \text{ , and} \qquad (40c)$$

$$B_p' = b_1 - 2b_2^e + 3b_3 \text{ .} \qquad (40d)$$

Unless the coefficients A_p'' and B_p'' are identically zero, P will not, in general, approach zero as $\rho \rightarrow 0$.

An analytic solution of Eq. (1) can be obtained in the limit of $\rho << \rho_0$ using the definition of the pressure given in Eq. (39). In this limit and assuming that A_p'' and B_p'' are not zero, the energy and density along an isentrope are related as

$$\exp(-B_p'' \rho_0 / \rho) = K (A_p'' + B_p'' \rho_0 \varepsilon) , \qquad (41)$$

where K is a constant along a given isentrope. In the limit as $\rho \rightarrow 0$, the LHS of Eq. (41) approaches zero (for $B_p'' > 0$). For the RHS of Eq. (41) to also approach zero in that limit, the energy will be

$$\varepsilon = -A_p'' / (B_p'' \rho_0) . \qquad (42)$$

Substituting the relation between energy and density of Eq. (41) into Eq. (39) gives a relation for the pressure along an isentrope for $\rho << \rho_0$,

$$P = K \exp(-B_p'' \rho_0 / \rho) . \qquad (43)$$

As $\rho \rightarrow 0$, the pressure approaches zero. The sound speed, in the low-density limit and assuming that A_p'' and B_p'' are not zero, can be written as

$$c^2 = [(A_p' + B_p' \rho_0 \varepsilon) / \rho_0] + [(A_p'' + B_p'' \rho_0 \varepsilon) (B_p'' \rho_0) / \rho^2] . \qquad (44)$$

The second term in Eq. (44) approaches zero but the first term remains nonzero as $\rho \rightarrow 0$.

If the polynomial EOS coefficients are chosen so that A_p'' and B_p'' are zero, the energy and density along an isentrope are related as

$$\rho / \rho_0 = K (A_p' + B_p' \rho_0 \varepsilon)^{\beta} , \qquad (45)$$

where $\beta = 1 / B_p'$ and K is a constant along a given isentrope. In the limit as $\rho \rightarrow 0$, the LHS of Eq. (45) approaches zero. The RHS of Eq. (45) will also approach zero ($\beta > 0$) if in that limit the energy becomes

$$\varepsilon = -A_p' / (B_p' \rho_0) . \qquad (46)$$

Substituting the relation between energy and density of Eq. (45) into Eq. (39) gives a relation for the pressure along an isentrope for $\rho << \rho_0$,

$$P = K (\rho / \rho_0)^{1/\beta} . \qquad (47)$$

As $\rho \rightarrow 0$, the pressure approaches zero. The sound speed, in the low-density limit and assuming A_p'' and B_p'' are zero, can be written as

$$c^2 = [(A_p' + B_p' \rho_0 \varepsilon) (1 + B_p') / \rho_0] . \qquad (48)$$

The sound speed goes to zero as $\rho \rightarrow 0$ for this choice of coefficients.

This approximate analysis indicates that the energy approaches a nonzero limit as $\rho \rightarrow 0$ whether the coefficients are chosen so that A_p'' and B_p'' are zero or nonzero. The pressure also approaches zero in this limit. The sound speed does not

approach zero if the coefficients are chosen so that A_p" and B_p" are nonzero but does approach zero if A_p" and B_p" are zero. However, it will be seen below that the numerical behavior of the polynomial EOS along an expansion isentrope differs significantly depending on whether A_p" and B_p" are zero or nonzero.

Numerical Expansion Isentropes

To perform numerical integrations of Eq. (1) it will be necessary to choose values of the coefficients a_i and b_i. Appendix A contains two sets of coefficients for Al for the polynomial EOS. In one set (called free), no restrictions were placed on the individual coefficients. For this choice, the values of A_p" and B_p" are nonzero. In the second set (called constrained) the coefficients were chosen such that

$$a_2^e = a_1 + a_3 \text{ , and} \tag{49a}$$

$$b_2^e = b_1 + b_3 - b_0 \text{ .} \tag{49b}$$

This choice forces A_p" and B_p" to be identically zero and P and $(\partial P/\partial \varepsilon)_\rho$ approach zero as $\rho \rightarrow 0$.

Figures 10 - 12 show plots of energy, pressure, and sound speed as a function of density along an expansion isentrope through a point on the Hugoniot at P = 10 Mbar (ρ = 7.091 g/cm^3 and e = 1.1552 Mbar-cm^3/g). The four curves in each plot show results from the Euler and ABM-PC methods using free and constrained coefficient sets. For energy (Fig. 10), the Euler integration using the free coefficients experiences large fluctuations starting at a density of ~0.004 g/cm^3. The ABM-PC integration using these coefficients stopped at a density of ~0.001 g/cm^3 with an indication that the differential equation became too stiff to continue. If an attempt is made to push the ABM-PC method to lower densities by relaxing the error tolerance, large fluctuations in energy are ultimately encountered. When the constrained coefficients were used, the Euler and ABM-PC integrations continued to a density of ~1.0x10^{-9} g/cm^3 without apparent problems. The behavior of the pressure (Fig. (11)) is similar to that of the energy. The sound speed calculated with the free coefficients using the ABM-PC integration shows fluctuations starting at a density of ~0.02 g/cm^3; these fluctuations become large at a density of ~0.003 g/cm^3, about the same density at which large fluctuations in the sound speed calculated by the Euler method begin. Sound speeds calculated with the constrained coefficients are negative but well behaved to densities of ~1.0x10^{-9} g/cm^3.

As with the Los Alamos EOS, the two ways of defining coefficients in the expansion region lead to significantly different behavior of ε, P, and c^2 at densities below ρ_0. A comparison of the results for this isentrope using the constrained coefficients with tabular EOS data (Holian 1984) for Al is given in Appendix B.

MIE-GRÜNEISEN - LINEAR Us-Up EOS

The Mie-Grüneisen - linear Us-Up EOS defines P as a function of ε and ρ by using a linear Us-Up Hugoniot of a material as a reference state and by defining states off the Hugoniot using the Mie-Grüneisen approximation (Harvey 1986). The linear Us-Up relation relates shock velocity (Us) to particle velocity (Up) as

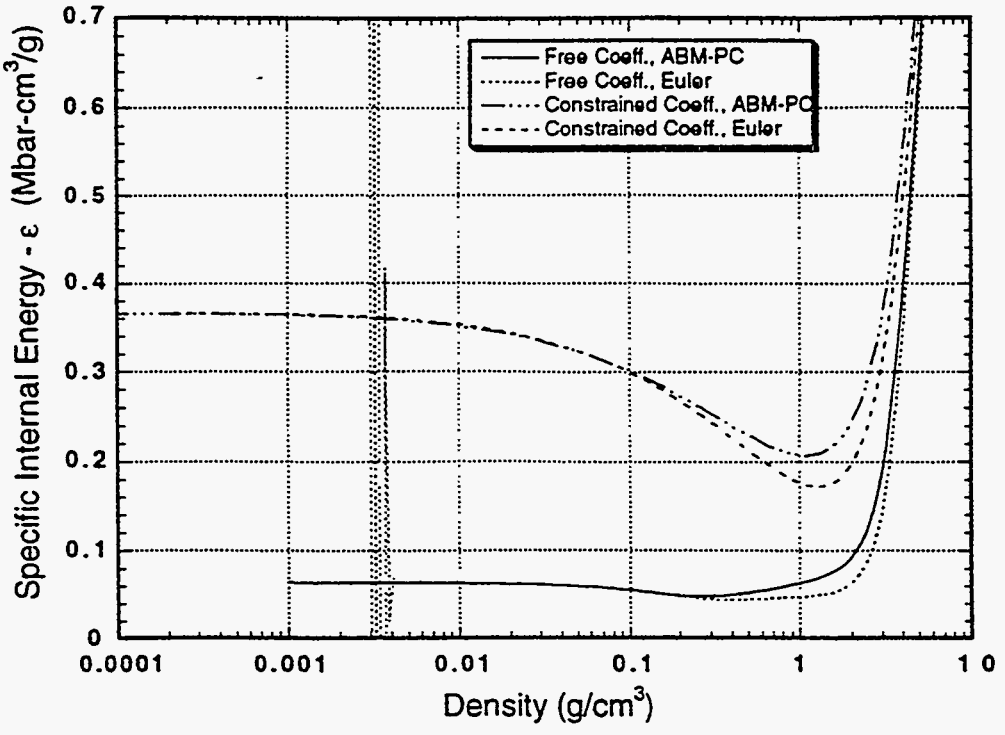

Fig. 10. Specific internal energy (ε) as a function of density (ρ) along an isentrope through 10 Mbar on the Hugoniot for a polynomial EOS for Al.

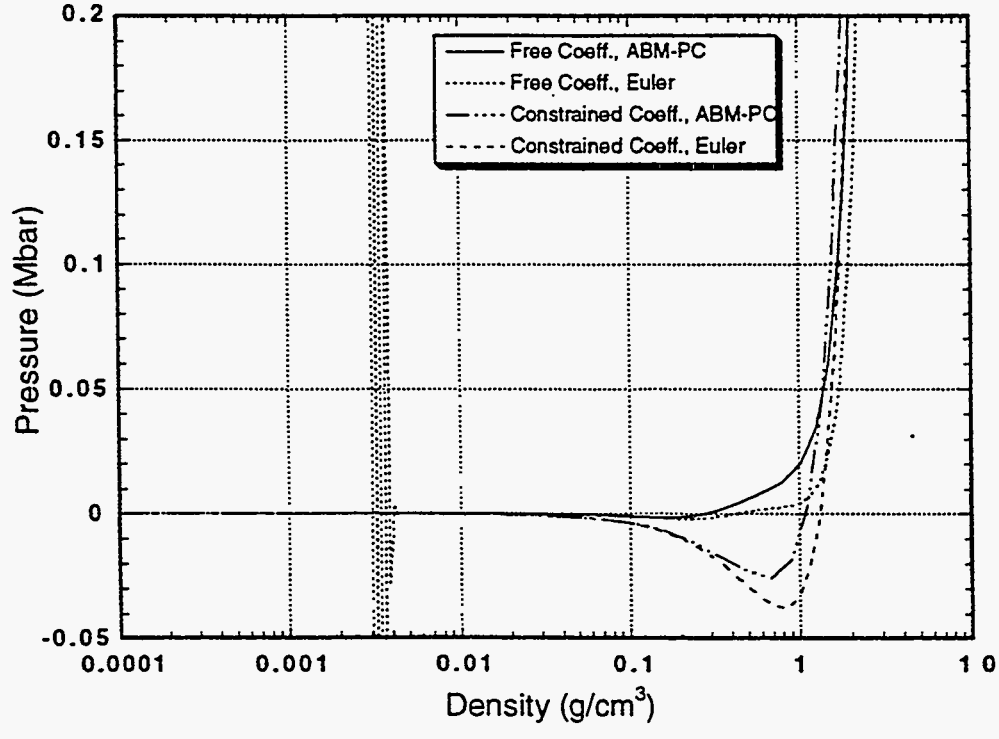

Fig. 11. Pressure (P) as a function of density (ρ) along an isentrope through 10 Mbar on the Hugoniot for a polynomial EOS for Al.

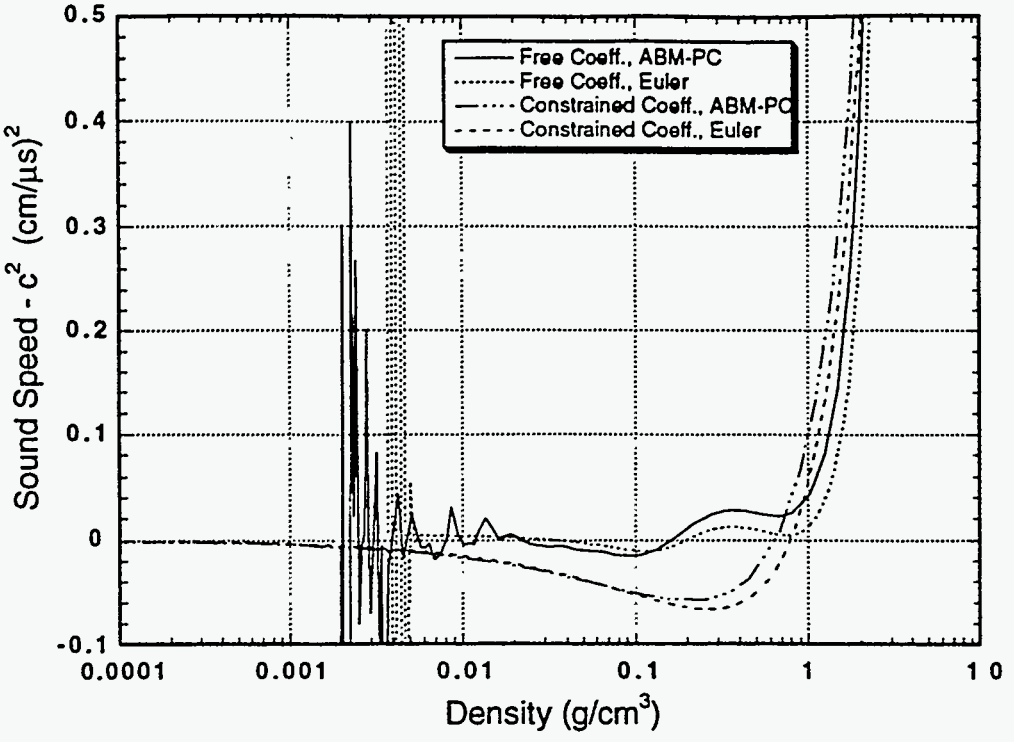

Fig. 12. Sound speed (c^2) as a function of density (ρ) along an isentrope through 10 Mbar on the Hugoniot for a polynomial EOS for Al.

$$Us = c_0 + s\,Up\ , \tag{50}$$

where c_0 and s are constants. From this, the pressure along the Hugoniot (P_H) is given by

$$P_H = \rho_0 c_0^2 \eta / (1 - s\eta)^2\ , \tag{51}$$

assuming a zero initial pressure. The quantity η is defined as $\eta = [1 - (\rho_0/\rho)]$. Defining a Grüneisen parameter Γ as $\rho\Gamma = (\partial P/\partial\varepsilon)_\rho$, the pressure relative to a reference state (P_r, ε_r) can be calculated as (Harvey 1986)

$$P = P_r + \rho\,\Gamma\,(\varepsilon - \varepsilon_r)\ . \tag{52}$$

Assuming a linear Us-Up Hugoniot as a reference state, the EOS is

$$P = \rho\,\Gamma\,\varepsilon + [\,\rho_0 c_0^2 \eta / (1 - s\eta)^2\,] - [\,\rho\,\Gamma\,c_0^2\,\eta^2 / 2\,(1 - s\eta)^2\,]\ . \tag{53}$$

Equations (51) and (53) have a problem for compression states ($\rho > \rho_0$), where P becomes infinite for $s\eta = 1$ or $\rho = \rho_0\, s / (s - 1)$. This problem can also lead to numerical difficulties during a calculation with strong compression. It has not been considered here.

The sound speed of the Mie-Grüneisen - linear Us-Up EOS is (Harvey 1986)

$$c^2 = \{ (\rho_0 c_0 / \rho)^2 [1 + s\eta + (s\eta^2 \Gamma \rho / \rho_0)] / (1 - s\eta)^3 \} + Z\{ \varepsilon - [(c_0^2 \eta^2) / 2 (1 - s\eta)^2] \} , \quad (54)$$

where

$$Z = [(d (\Gamma \rho)/d \rho] + (\Gamma\rho / \rho)^2 . \quad (55)$$

The quantity Γ is assumed not to be a function of ε but may be a function of ρ. Some common functional forms used are

$$\Gamma = \Gamma_0 , \quad (56a)$$

$$\rho \Gamma = \rho_0 \Gamma_0 , \text{ and} \quad (56b)$$

$$\rho \Gamma = \rho_0 \Gamma_0 / (1 + \eta \Gamma_0) , \quad (56c)$$

where Γ_0 is a constant. The third form (Eq. (56c)) has a problem in that Γ becomes infinite when $\eta = -1 / \Gamma_0$ ($\rho/\rho_0 = \Gamma_0 / [1 + \Gamma_0]$) and is negative for lower densities. For normal values of Γ_0 (~1.5-3), this occurs for densities of 60-75% of normal density. Thus, Eq. (56c) is not a viable definition for Γ when significant expansions are possible. It was not considered further here. Equation (56b) is the preferred definition of Γ for calculations involving compression. Using Γ defined by Eq. (56a) does not represent high-density data off the Hugoniot well. From the definition of Γ, $(\partial P/\partial \varepsilon)_\rho \rightarrow 0$ as $\rho \rightarrow 0$ for Eq. (56a), but $(\partial P/\partial \varepsilon)_\rho = \rho_0 \Gamma_0$ (a constant) for Eq. (56b).

As with the Los Alamos and polynomial EOSs, the Mie-Grüneisen - linear Us-Up EOS does not have an analytic solution for an isentrope. It is possible to obtain an analytic solution for one choice of Γ in the limit for $\rho << \rho_0$.

Behavior in the Low-Density Limit

For $\rho << \rho_0$, Eq. (53) can be approximated by

$$P = \rho \Gamma \varepsilon - \rho c_0^2 (1 + \Gamma/2) / s^2 . \quad (57)$$

The behavior of this EOS along an isentrope depends on the variation of Γ with ρ. For Γ defined by Eq. (56a), an analytic solution to Eq. (1) in this limit is

$$\rho^{\Gamma_0} = K (\Gamma_0 \varepsilon - c_0^2 (1 + \Gamma_0/2) / s^2) , \quad (58)$$

where K is a constant along a given isentrope. In the limit as $\rho \rightarrow 0$ the LHS of Eq. (58) approaches zero since $\Gamma_0 > 0$. For the RHS of Eq.(58) to approach zero, the energy becomes

$$\varepsilon = c_0^2 (1 + \Gamma_0/2) / \Gamma_0 s^2 . \quad (59)$$

In the limit as $\rho \rightarrow 0$, the pressure and sound speed also approach zero along an isentrope for this definition of Γ.

A closed-form analytic solution was not found for Eq. (1) in the low density limit when Γ was defined by Eq. (56b). A solution involving an infinite series in density indicated that as $\rho \rightarrow 0$, the energy becomes

$$\varepsilon = c_0^2 / 2 s^2 \ . \qquad (60)$$

Relations for the pressure and sound speed were not found for this definition of Γ.

This approximate analysis indicates that the energy approaches a nonzero limit as $\rho \rightarrow 0$ for both definitions of Γ considered (Eqs. (56a) and (56b)). The pressure and sound speed also approaches zero in this limit for Eq. (56a). However, it will be seen below that the numerical behavior of the Mie-Grüneisen - linear Us-Up EOS along an expansion isentrope can be erratic for Γ defined by Eq. (56b).

Numerical Expansion Isentropes

To perform numerical integrations of Eq. (1) it will be necessary to choose values of the coefficients c_0, s and Γ_0 , and a relation for Γ. Appendix A contains values of c_0, s, and Γ_0 for Al. Figures 13 - 15 show plots of energy, pressure, and sound speed as a function of density along an expansion isentrope through a point on the Hugoniot at P = 10 Mbar (ρ = 6.519 g/cm^3 and ε = 1.0852 Mbar-cm^3/g). The four curves in each plot show results from the Euler and ABM-PC methods using Eqs. (56a) and (56b) as definitions of Γ. For energy (Fig. 13), the Euler integration using the Eq. (56b) definition experiences large fluctuations starting at a density of ~0.03 g/cm^3. The ABM-PC integration using these coefficients stopped at a density of ~0.01 g/cm^3 with an indication that the differential equation became too stiff to continue. As noted for the other EOSs, if an attempt is made to push the ABM-PC method to lower densities by relaxing the error tolerance, large fluctuations in energy are ultimately encountered. When Eq. (56a) is used, the Euler and ABM-PC integrations continued to a density of ~1.0x10^{-9} g/cm^3 without apparent problems. The behavior of the pressure (Fig. (14)) is similar to that of the energy. The sound speed calculated with Eq. (56b) using the ABM-PC integration shows fluctuations starting at a density of ~0.2 g/cm^3; these fluctuations become large at a density of ~0.02 g/cm^3, about the same density at which large fluctuations in the sound speed calculated by the Euler method begin. Sound speeds calculated with Γ defined by Eq. (56a) are negative but well behaved to densities of ~1.0x10^{-9} g/cm^3.

There is little difference between the behavior of P (Fig. (14)) or c^2 (Fig. (15)) at densities less than ρ_0 for the two methods of defining Γ. Only the limiting values of ε (Fig. (13)) are significantly different. A comparison of the results for this isentrope using the Eq. (56a) coefficients with tabular EOS data (Holian 1984) for Al is given in Appendix B.

DISCUSSION

During modeling of impacts, it often occurs that one or more materials expands to low density after being shocked. Under these circumstances, unrealistic values of specific internal energy (ε), pressure (P), or sound speed squared (c^2) can be calculated for some analytic EOSs as the density becomes small relative to the normal or reference density. These unrealistic values of material properties can lead

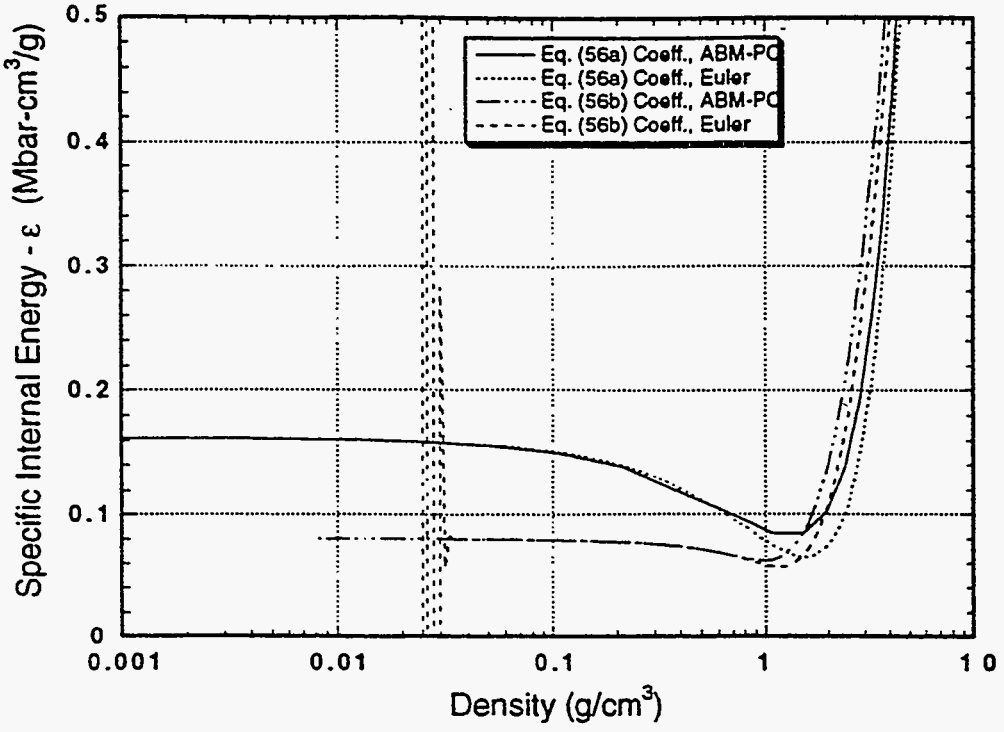

Fig. 13. Specific internal energy (ε) as a function of density (ρ) along an isentrope through 10 Mbar on the Hugoniot for a Mie-Grüneisen EOS for Al.

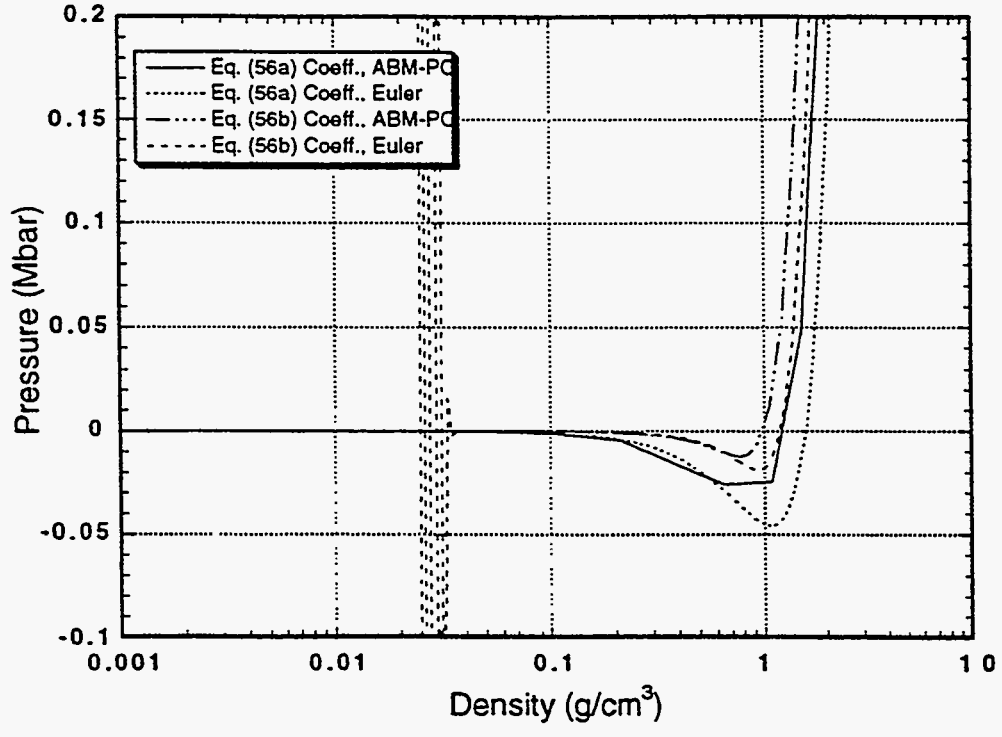

Fig. 14. Pressure (P) as a function of density (ρ) along an isentrope through 10 Mbar on the Hugoniot for a Mie-Grüneisen EOS for Al.

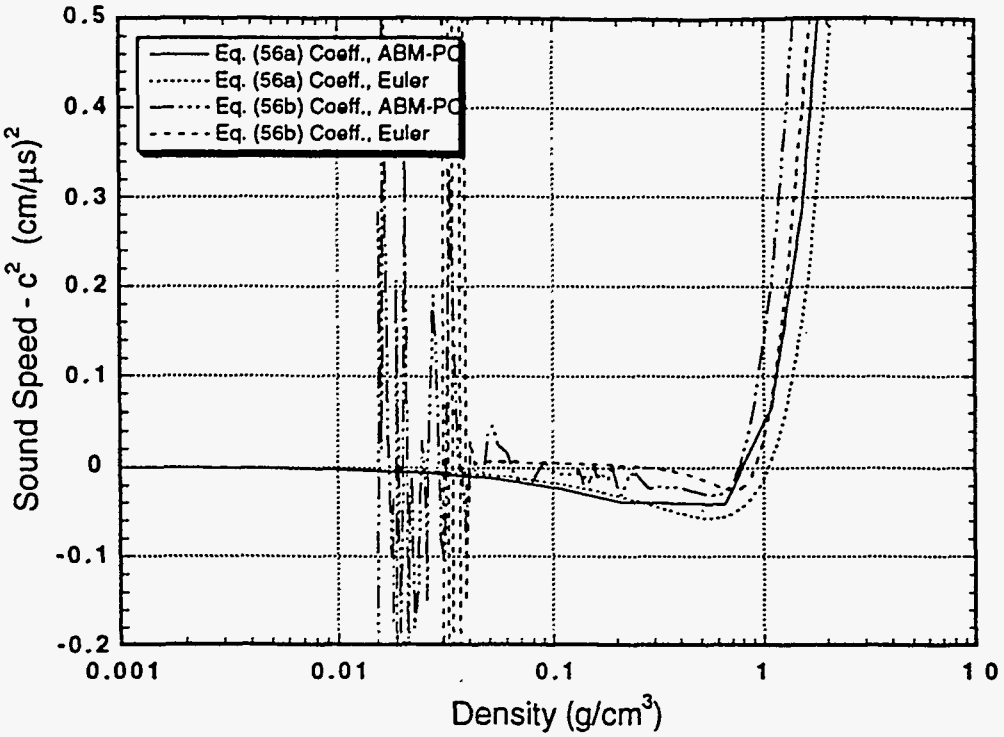

Fig. 15. Sound speed (c^2) as a function of density (ρ) along an isentrope through 10 Mbar on the Hugoniot for a Mie-Grüneisen EOS for Al.

to small time steps or large material velocities that slow or stop a calculation. This behavior has been observed for three analytic EOSs during MESA-2D calculations. These EOSs are the Los Alamos EOS, the MESA polynomial EOS, and a Mie-Grüneisen EOS based on a linear relation between shock and particle velocity.

An expansion process that is simulated in hydrodynamic calculations in which strength and viscosity effects are not modeled should occur isentropically. For a variety of reasons, such calculations do not always maintain the isentropic nature of the expansion process. Deviations from isentropic conditions can often be traced to the interplay of the EOS and the numerical schemes implemented in the hydrodynamic code. When the EOS is not well behaved in the low-density region, the computational results can be catastrophic. It is important to understand the behavior of an EOS as the differential equation defining an isentrope is integrated analytically (if possible) and numerically. The time-step procedure used in hydrocode calculations is effectively a numerical-integration process. Although an EOS can show a well-behaved analytic isentrope in the low-density limit, numerical integration can lead to large deviations of the energy, pressure, or sound speed from realistic values.

Analytic and numerical solutions for isentropes for three simple analytic EOSs have been compared. This comparison provides insight into the difficulties that can arise in the numerical solutions. Approximate analytic solutions (for $\rho << \rho_0$) and numerical solutions for isentropes for the three more-realistic EOSs have also been discussed. Table I summarizes the behavior of isentropic expansions of all these EOSs in the limit as $\rho \rightarrow 0$. The term "erratic" used for some entries indicates either

that large fluctuations occur in the value or that the differential equation becomes too stiff to continue (ABM-PC method). Question marks are associated with entries that have not been determined analytically.

Of the three simplified EOSs for which analytic solutions for an isentrope are available, the ideal gas EOS (Eq. (6)) represents an ideal situation in which energy, pressure, and sound speed all approach zero as $\rho \rightarrow 0$. The EOS is also well behaved numerically. The analytic solution for an isentrope for the stiffened gas EOS (Eq. (11)) indicates that the energy becomes infinite, the pressure approaches a finite but nonzero value, and the sound speed approaches zero as $\rho \rightarrow 0$. Numerical solutions for the stiffened gas EOS show similar behavior for the energy and pressure, but $c^2 \rightarrow \pm\infty$ depending on the numerical scheme (see Figs. 1-3). This problem with the numerical calculation of the sound speed occurs because the analytic limit for sound speed along an isentrope results from the cancellation of terms that become infinite as $\rho \rightarrow 0$. The energy and density evaluated numerically are only approximations to the analytic isentrope and the exact cancellation does not occur. The infinite limit for the energy of the stiffened gas EOS as $\rho \rightarrow 0$ is unrealistic. The modified stiffened gas EOS (Eq. (16)) remedies this problem, giving a finite (but nonzero) limit for the energy and a zero limit for the pressure and sound speed as $\rho \rightarrow 0$ for the analytic solution for an isentrope. However, a price is paid in that the numerical results are all erratic for this EOS. A major difference between these EOSs is that $(\partial P/\partial \varepsilon)_\rho$ approaches zero for the stiffened gas EOS as $\rho \rightarrow 0$, but $(\partial P/\partial \varepsilon)_\rho$ approaches a nonzero value ($b_0\, \rho_0$) in that limit for the modified stiffened gas EOS. The nonzero limit of $(\partial P/\partial \varepsilon)_\rho$ leads to a differential equation that becomes very stiff or unstable as $\rho \rightarrow 0$. The ABM-PC method recognizes the stiffness of the differential equation and stops the numerical integration; the Euler method does not stop and produces large fluctuations in the variables (see Figs. 4-6).

The Los Alamos EOS (Eq. (21)) is used to model solids. In the limit as $\rho \rightarrow 0$ the analytic solution for the energy along an isentrope approaches a finite (but nonzero) value. Limiting analytic values for the pressure and sound speed were not obtained because of the complexity of the energy-density relation along an isentrope. The numerical behavior of the Los Alamos EOS depends on the choice of coefficients. When no attempt is made to force the pressure and $(\partial P/\partial \varepsilon)_\rho$ to approach zero as $\rho \rightarrow 0$ (Eqs. (33) definition of the expansion-region quadratic coefficients), the numerical behavior of the energy, pressure, and sound speed is quite erratic in that limit (see Figs. 7-9). The onset of irregular behavior depends on the numerical method used. The Euler method shows erratic behavior before the ABM-PC method stops because the differential equation is too stiff. When the pressure and $(\partial P/\partial \varepsilon)_\rho$ are forced to zero as $\rho \rightarrow 0$ (Eqs. (34) definition of the expansion-region quadratic coefficients), the numerical solutions are well behaved in this limit (see Figs. 7-9). The erratic behavior seen in the numerical solutions for an isentrope when the Eqs. (33) definitions of the coefficients are used is the same as seen in hydrodynamic calculations with this definition of the coefficients. Large positive or negative values of the energy, pressure, or sound speed squared occur in some cells with low-density material. Time steps become very small if the sound speed becomes large or material velocities can become unrealistically large if the pressure becomes large. These symptoms require user efforts to try to correct them, if corrections are possible, while maintaining the same definitions of the coefficients. By redefining the expansion-region quadratic coefficients according to Eqs. (34), the

Table I. Summary of the limiting behavior of isentropic expansions for various equations of state.

EOS	Limit as $\rho \rightarrow 0$ for an Isentrope					
	Analytical			Numerical		
	ε	P	c^2	ε	P	c^2
Ideal Gas	0	0	0	0	0	0
Stiffened Gas	∞	finite but nonzero	0	∞	finite but nonzero	$\pm\infty$
Modified Stiffened Gas	finite but nonzero	0	0	erratic	erratic	erratic
Los Alamos Eqs. (33) Coeff.	finite but nonzero	0 (?)	0 (?)	erratic	erratic	erratic
Los Alamos Eqs. (34) Coeff.	finite but nonzero	0	0 (?)	finite but nonzero	0	0
Polynomial Free Coeff.	finite but nonzero	0	finite and nonzero	erratic	erratic	erratic
Polynomial Constrained Coeff.	finite but nonzero	0	0	finite but nonzero	0	0
Mie-Grüneisen Eq. (56a) Coeff.	finite but nonzero	0	0	finite but nonzero	0	0
Mie-Grüneisen Eq. (56b) Coeff.	finite but nonzero	0 (?)	0 (?)	erratic	erratic	erratic

EOS produces well-behaved values of energy, pressure, and sound speed in the low-density region.

The behavior of the polynomial EOS (Eq. (35)) is similar to that of the Los Alamos EOS. The free coefficients for the polynomial EOS are analogous to the Eqs. (33) coefficients for the Los Alamos EOS. Although the analytic behavior of this EOS is acceptable, when the free coefficients are used, erratic behavior of the energy, pressure, and sound speed is seen for numerical solutions in the limit as $\rho \rightarrow 0$. By constraining the coefficients so that pressure and $(\partial P/\partial \varepsilon)_\rho$ approach zero as $\rho \rightarrow 0$, the numerical solutions for an isentrope are well behaved in that limit.

The Mie-Grüneisen EOS based on a linear relation between shock and particle velocity is well behaved in the limit as $\rho \rightarrow 0$ if Eq. (56a) is used to define Γ.

However, this definition does not represent compression states ($\rho > \rho_0$) off the Hugoniot well. Using Eq. (56b) to define Γ describes compressions states well, but results in erratic behavior of numerical solutions as $\rho \rightarrow 0$. A solution to this difficulty would be to use Eq. (56b) to define Γ for $\rho > \rho_0$ and Eq. (56a) to define Γ for $\rho < \rho_0$. In this case the pressure would be continuous across this boundary but the sound speed would not. Alternate definitions of Γ for $\rho < \rho_0$ could be devised so that the sound speed would also be continuous. An example is

$$\rho\,\Gamma = \rho_0\,\Gamma_0\,(\rho/\rho_0)\,[\,2 - (\rho/\rho_0)\,] \quad . \tag{61}$$

This definition makes Z (Eq. (55)) and the sound speed continuous across the ρ_0 boundary. In the limit as $\rho \rightarrow 0$, $\Gamma \rightarrow 2\,\Gamma_0$, $P \rightarrow 0$, and $(\partial P/\partial \varepsilon)_\rho \rightarrow 0$.

Table II lists values of $(\partial P/\partial \varepsilon)_\rho$ and the limits of P and $(\partial P/\partial \varepsilon)_\rho$ as $\rho \rightarrow 0$, for the various EOSs discussed here. The limit of the pressure shown in Table II is a limit in general and not necessarily along an isentrope as was shown in Table I. If the limit of P as $\rho \rightarrow 0$ is a function of ε, it follows that the limit of $(\partial P/\partial \varepsilon)_\rho$ is nonzero. Comparing the results of Tables I and II, whenever the numerical behavior of ε, P, and c^2 along an isentrope was erratic in the limit as $\rho \rightarrow 0$ (see Table I), $(\partial P/\partial \varepsilon)_\rho$ was nonzero in the limit as $\rho \rightarrow 0$ (see Table II). For the Los Alamos, polynomial, and Mie-Grüneisen EOSs, requiring the limit of P as $\rho \rightarrow 0$ to be zero in general also forced $(\partial P/\partial \varepsilon)_\rho$ to be zero in that limit. The behavior of $(\partial P/\partial \varepsilon)_\rho$ in the limit as $\rho \rightarrow 0$ is a measure of the stability of the numerical integration of Eq. (1) in that limit (Gear 1971). Controlling P in that limit is a convenient method of controlling $(\partial P/\partial \varepsilon)_\rho$.

The analysis presented here has highlighted a fundamental problem with some analytic EOSs when expansions to densities much less than the reference or normal density are encountered in hydrodynamic calculations. With the present structure of MESA-2D, the user can eliminate this problem for the Los Alamos and polynomial EOSs by the proper choice of coefficients in the expansion region. For the Los Alamos EOS, use Eqs. (34) to define a_2^e, b_2^e, and c_2^e in terms of the other coefficients. Existing compilations of coefficients for the Los Alamos EOS normally use Eqs. (33) to define these coefficients. Thus, a user who wishes to follow the recommendations made here may have to evaluate these three coefficients for himself. For the polynomial EOS, use Eqs. (49) to define a_2^e and b_2^e in terms of the other coefficients. For the polynomial EOS that was obtained for Al (see Appendix A), this constraint was applied during the process of fitting the polynomial form to Al data.

For the Mie-Grüneisen EOS, there is no mechanism to change the definition of Γ when the density drops below the normal density. Adding this option to MESA-2D should ease the problems encountered with this EOS when materials expand to very low densities.

Table II. Summary of the limiting behavior of pressure and $(\partial P/\partial \varepsilon)_\rho$ as $\rho \rightarrow 0$ for various equations of state.

EOS	limit of P as $\rho \rightarrow 0$ in general	$(\partial P/\partial \varepsilon)_\rho$	limit as $\rho \rightarrow 0$ $(\partial P/\partial \varepsilon)_\rho$
Ideal Gas	0	$(\gamma - 1)\,\rho$	0
Stiffened Gas	nonzero but constant	$(\gamma - 1)\,\rho$	0
Modified Stiffened Gas	function of ε	$b_0\,\rho_0 + b_1\,\rho$	nonzero
Los Alamos Eqs. (33) Coeff.	function of ε	$[B_o(\mu)\rho_0 + C_o(\mu)\varepsilon\,\rho_0^2] / Q - P\,\rho_0 / Q^2$	nonzero
Los Alamos Eqs. (34) Coeff.	0	$[B_o(\mu)\rho_0 + C_o(\mu)\varepsilon\,\rho_0^2] / Q - P\,\rho_0 / Q^2$	0
Polynomial Free Coeff.	function of ε	$B_p(\mu)\rho_0$	nonzero
Polynomial Constrained Coeff.	0	$B_p(\mu)\rho_0$	0
Mie-Grüneisen Eq. (56a) Coeff.	0	$\rho\,\Gamma$	0
Mie-Grüneisen Eq. (56b) Coeff.	function of ε	$\rho\,\Gamma$	nonzero

REFERENCES

C. W. Gear, *Numerical Initial Value Problems in Ordinary Differential Equations*, (Prentice-Hall Inc., Englewood Cliffs, NJ, 1971).

F. H. Harlow and A. A. Amsden, "Fluid Dynamics," Los Alamos Scientific Laboratory report LA-4700 (June 1971).

W. B. Harvey, "Attenuation of Shock Waves in Copper and Stainless Steel," Ph. D. thesis submitted to the Dept. of Physics, New Mexico State Univ., Las Cruces, NM; Los Alamos National Laboratory report LA-10753-T (June 1986).

K. S. Holian, "T-4 Handbook of Material Properties Data Bases, Vol. 1c: Equations of State", Los Alamos National Laboratory report LA-10160-MS (November 1984).

L. F. Shampine and H. A. Watts, "DEPAC - design of a user oriented package of ODE solvers," Sandia National Laboratory report SAND79-2374 (September 1980).

J. A. Zukas, T. Nicholas, H. F. Swift, L. B. Greszczuk, and D. R. Curran, *Impact Dynamics*, (John Wiley and Sons, New York, NY, 1982) p. 443-444.

APPENDIX A

VALUES OF COEFFICIENTS USED IN NUMERICAL INTEGRATIONS

The different EOS forms investigated here use a variety of coefficients to define the behavior of pressure as a function of density and specific internal energy. The values used in numerical calculations are listed here. For all the EOSs, $\rho_0 = 2.7$ g/cm^3 .

Stiffened Gas EOS

The coefficients in Eq. (11) are:

$\gamma = 2.5$, and $\quad a = 0.3$.

Modified Stiffened Gas EOS

The coefficients in Eq. (16) are:

$b_0 = 1.5$, $\quad b_1 = 1.0$, and

$a = 0.3$.

Los Alamos EOS

The coefficients in Eqs. (21) and (22), using the Eq. (33) definition, are:

$a_1 = 1.1867466$, $\quad a_2^c = 0.762995$,

$a_2^e = -0.762995$, $\quad b_0 = 3.4447654$,

$b_1 = 1.5450573$, $\quad b_2^c = 0.96429632$,

$b_2^e = 0.96429632$, $\quad c_0 = 0.43381656$,

$c_1 = 0.54873462$, $\quad c_2^c = 0.0$,

$c_2^e = 0.0$, and $\quad \varepsilon_0 = 1.5$.

The coefficients in Eqs. (21) and (22), using the Eq. (34) definition, are:

$a_1 = 1.1867466$, $\quad a_2^c = 0.762995$,

$a_2^e = 1.1867466$, $\quad b_0 = 3.4447654$,

$b_1 = 1.5450573$, $\quad b_2^c = 0.96429632$,

$b_2^e = -1.8997081$, $\quad c_0 = 0.43381656$,

$c_1 = 0.54873462$, $\quad c_2^c = 0.0$,

$c_2^e = 0.11491806$, and $\quad \varepsilon_0 = 1.5$.

Polynomial EOS

The free coefficients in Eqs. (35) and (36) are:

$a_1 = 0.4092909$, $a_2^c = 0.5032754$,
$a_2^e = 0.8517608$, $a_3 = 0.4829053$,
$b_0 = 2.046899$, $b_1 = 5.058369$,
$b_2^c = -5.672175$, $b_2^e = 4.643042$, and
$b_3 = 1.397754$.

The constrained coefficients in Eqs. (35) and (36) are:

$a_1 = 0.745844$, $a_2^c = 0.7194863$,
$a_2^e = 0.8287573$, a3 = 0.08291327,
$b_0 = 1.113364$, $b_1 = 1.970801$,
$b_2^c = -1.50121$, $b_2^e = 1.268511$, and
$b_3 = 0.4110738$.

Mie-Grüneisen EOS based on a linear relation between shock and particle velocity

The coefficients in Eqs. (53) and (56) are:

$c_0 = 0.5392$, $s = 1.341$, and
$\Gamma_0 = 2.0$.

APPENDIX B

COMPARISON OF ANALYTIC EOS RESULTS WITH TABULAR EOS DATA

The various analytic EOSs discussed here give different results for the specific internal energy (ε), pressure (P), and sound speed squared (c^2) in the expansion region. For the conditions shown in Figs. 1-15, there are no experimental data that could be used for comparison. A comparison was made between the isentropes of the stable-coefficient choices for the Los Alamos, polynomial, and Mie-Gruneisen EOSs and the same isentrope from a tabular EOS for Al, SESAME material number 3717 (Holian 1984). Figures B1 - B3 show plots of specific internal energy, pressure, and sound speed squared as a function of density for these four EOSs.

The SESAME isentrope indicates that ε asymptotes to a value of ~0.10 Mbar-cm^3/g at low density (see Fig. B1). The asymptote for the Los Alamos EOS is close to that value; the polynomial EOS asymptote is quite inaccurate. All three analytic EOSs show poor agreement with the SESAME result at densities of ~1-2 g/cm^3. The SESAME isentrope indicates that the pressure never becomes negative (see Fig. B2). All three analytic EOSs give negative pressures with the Los Alamos EOS being closest to the SESAME result. Similarly, c^2 is never negative along the SESAME isentrope, but all three analytic EOSs show negative values. Again the Los Alamos EOS is closest to the SESAME result in the expansion region.

The primary purpose of this work was to investigate the behavior of analytic EOSs in the low-density limit and to propose solutions to the problems found. The fact that none of the analytic EOSs examined here show good agreement with the SESAME results is incidental to this purpose, but important in itself. The Los Alamos and polynomial EOSs are empirical. The Mie-Grüneisen EOS has a physical basis, but not very sophisticated. To the extent that the physical basis for SESAME EOSs is reasonable, even outside areas where experimental data are available, this comparison would indicate that EOSs such as SESAME should be used in impact modeling whenever possible. The wide range of conditions that can be encountered (high compressions followed by expansions to low pressure) are difficult for an analytic EOS to cover accurately. However, there are situations where an analytic EOS will be used because a better choice is unavailable. In those situations, the behavioral problems of analytic EOS in the low-density limit that were described here should be recognized and eliminated where possible.

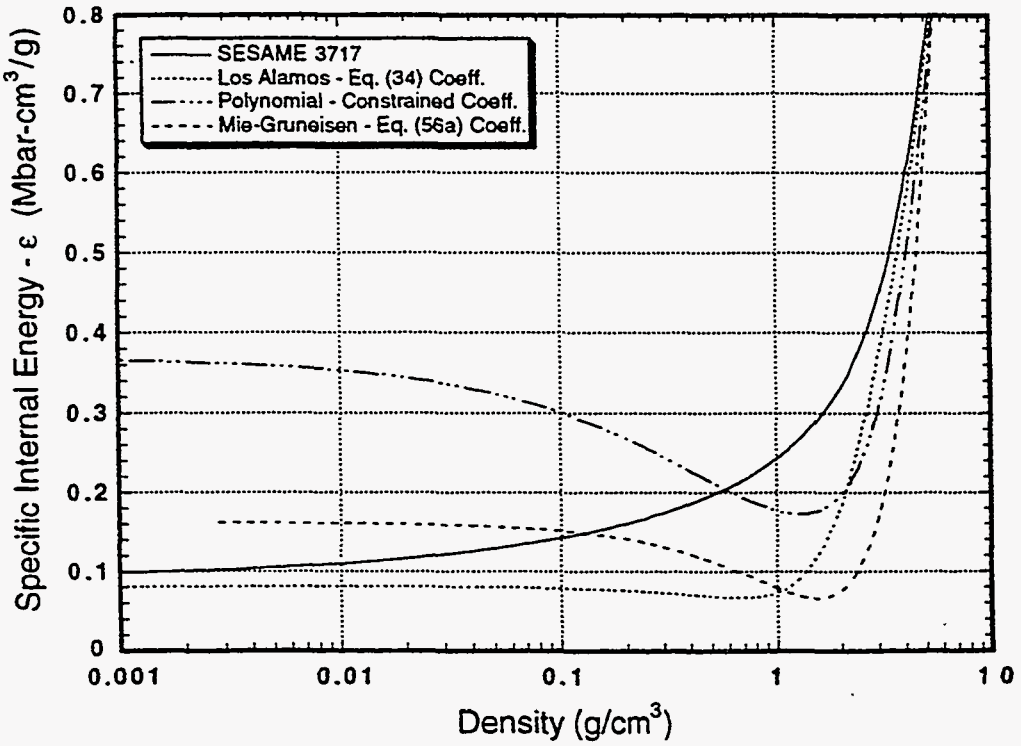

Fig. B1. Comparison of specific internal energy (ε) as a function of density (ρ) along an isentrope through 10 Mbar on the Hugoniot for four EOSs for Al.

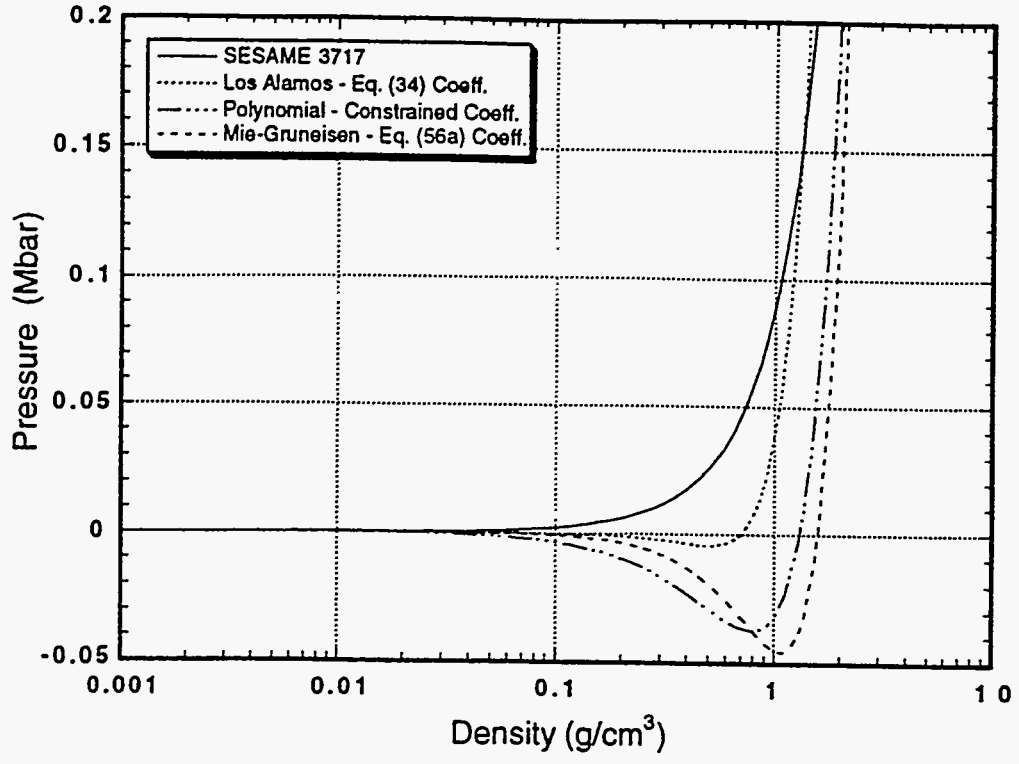

Fig. B2. Comparison of pressure (P) as a function of density (ρ) along an isentrope through 10 Mbar on the Hugoniot for four EOSs for Al.

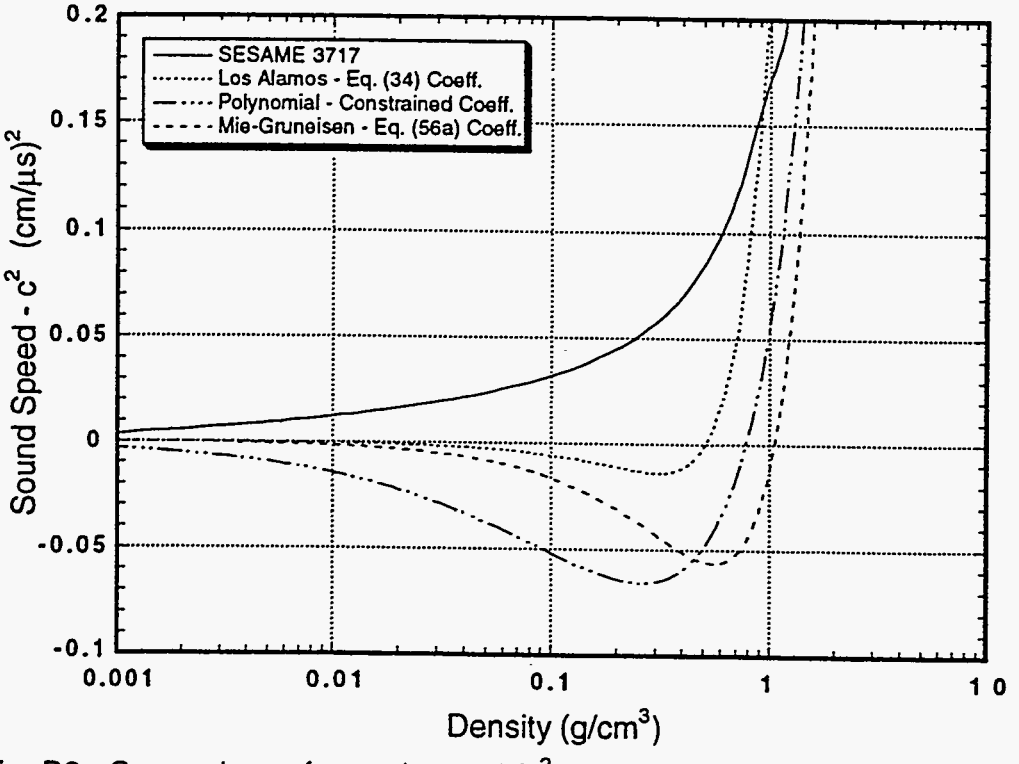

Fig. B3. Comparison of sound speed (c^2) as a function of density (ρ) along an isentrope through 10 Mbar on the Hugoniot for four EOSs for Al.